Advanced Fiber Materials (2022) 4:573–603
https://doi.org/10.1007/s42765-022-00133-y

REVIEW

Flexible Ceramic Fibers: Recent Development in Preparation and Application

Chao Jia[1] · Zhe Xu[1] · Dianfeng Luo[1] · Hengxue Xiang[1] · Meifang Zhu[1]

Received: 16 August 2021 / Accepted: 3 January 2022 / Published online: 11 February 2022

Abstract

Flexible ceramic fibers (FCFs) have been developed for various advanced applications due to their superior mechanical flexibility, high temperature resistance, and excellent chemical stability. In this article, we present an overview on the recent progress of FCFs in terms of materials, fabrication methods, and applications. We begin with a brief introduction to FCFs and the materials for preparation of FCFs. After that, various methods for preparation of FCFs are discussed, including centrifugal spinning, electrospinning, solution blow spinning, self-assembly, chemical vapor deposition, atomic layer deposition, and polymer conversion. Recent applications of FCFs in various fields are further illustrated in detail, including thermal insulation, air filtration, water treatment, sound absorption, electromagnetic wave absorption, battery separator, catalytic application, among others. Finally, some perspectives on the future directions and opportunities for the preparation and application of FCFs are highlighted. We envision that this review will provide readers with some meaningful guidance on the preparation of FCFs and inspire them to explore more potential applications.

Keywords Ceramic fibers · Flexibility · Preparation · Applications

Introduction

In recent years, ceramic fiber materials have been paid more and more attention, as can be seen from the number of published literatures. By searching the literature published on "ceramic fiber" in the core database of Web of Science in recent 10 years (2011–2020), it is found that the number of literatures on ceramic fiber materials is increasing (Fig. 1a). It should be noted that the reduction of literature in 2020 could be due to the COVID-19 outbreak. China is the origin of potteries and using ceramic materials. In addition, Chinese scientific technology and research centers are extremely focused on materials science and engineering, particularly in ceramic related subjects (Fig. 1b). During the past 10 years, China has published nearly 3000 publications in the field of ceramic fibers, which has been over 40% of the total number of universal publications in the same period. This rate of development stands far higher than that in United States, Germany, Japan, and other countries.

Traditional ceramic fiber materials are usually prepared from ceramic oxide particles, and the inherent brittleness of ceramic materials greatly limits their application. Flexible ceramic fibers (FCFs) are kind of fibrous lightweight refractory material, and they possess superior mechanical flexibility, high temperature resistance, and excellent chemical stability. Various methods have been developed for preparing FCFs, different benefits and characteristics. FCFs two-dimensional ceramic fiber, films and three-dimensional ceramic fiber aerogels usually possess low density, low thermal conductivity, large specific surface area and many other excellent properties. Due to the superior properties of FCFs, they have been widely used in the fields of thermal insulation [1–3], air filtration [4, 5], water treatment [6–8], sound absorption [3, 9], etc.

In this review, we focus on the latest advances in FCFs, including their material system, preparation methods and applications (Fig. 1c). We will first briefly introduce the materials used in the preparation of FCFs, including oxides, carbides, nitrides and so on. Various methods for fabrication of FCFs, including centrifugal spinning, electrospinning, solution blow spinning, self-assembly, chemical vapor

✉ Chao Jia
jiachao0806@dhu.edu.cn

[1] State Key Laboratory for Modification of Chemical Fibers and Polymer Materials, College of Materials Science and Engineering, Donghua University, Shanghai 201620, China

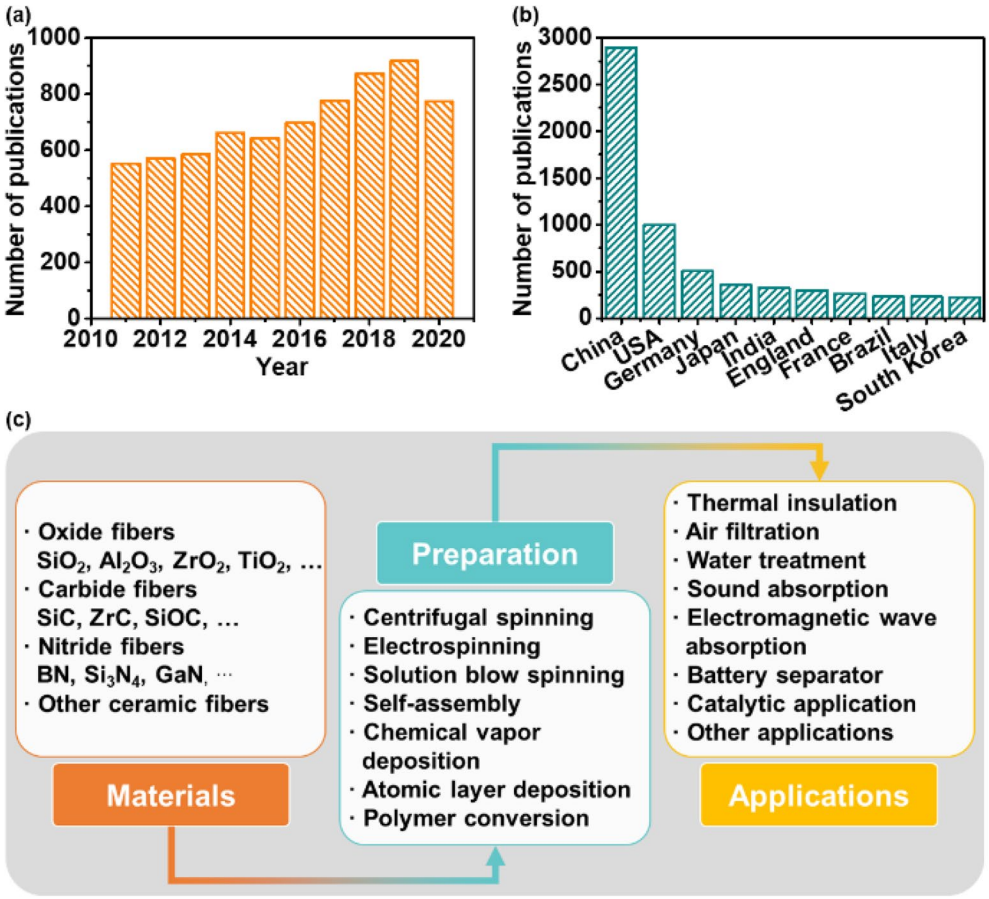

Fig. 1 Development status of ceramic fiber materials. **a** Number of literatures published annually during the period of 2011–2020 on the subject of "ceramic fiber" retrieved from the core database of Web of Science. **b** Number of publications for the top 10 countries in the last 10 years. **c** Research progress of FCFs in terms of materials, preparation methods and applications

deposition, atomic layer deposition, and polymer conversion are introduced. We also highlight the most recent applications of FCFs in thermal insulation, air filtration, water treatment, sound absorption, electromagnetic wave absorption, battery separator, and catalytic application. Finally, some perspectives on the future development of FCFs are provided.

Materials for Preparation of FCFs

Ceramic fibers can be divided into oxide fibers, carbide fibers, nitride fibers and other ceramic fibers, according to their chemical composition. Oxide fibers usually have high mechanical strength, low thermal conductivity, good electrical insulation and chemical stability, and can remain stable in the oxygen atmosphere. Some kinds of oxide ceramics such as, silica (SiO_2) [1, 10–20], alumina (Al_2O_3) [21–28], zirconia (ZrO_2) [2, 5, 29–33], titania (TiO_2) [2, 34–43], zinc oxide (ZnO) [17, 39, 44–47], mullite [48–53], cerium oxide (CeO_2) [54], nickel oxide (NiO) [55], cobalt oxide (Co_3O_4) [55], copper oxide (CuO) [17, 56], stannic oxide (SnO_2) [57], etc can be processed into FCFs. In addition, there are plenty of reports on hetero-elements and complex oxide ceramic fibers including $BaTiO_3$ fibers [2, 16, 58–60], $Li_{0.33}La_{0.56}TiO_3$ (LLTO) fibers [16, 61, 62], $Li_7La_3Zr_2O_{12}$ (LLZO) fibers [16], $CaCu_3Ti_4O_{12}$ fibers [63–65], $LiNi_{0.5}Mn_{1.5}O_4$ fibers [66], yttrium–aluminum-garnet (YAG) fibers [67], indium tin oxide (ITO) fibers [68, 69], YBCO fibers [70], MFe_2O_4 (M=Cu, Co, Ni) fibers [71], and so on.

Silicon carbide (SiC) fibers are the most common carbide fiber [6, 72–76]. Due to the strong covalent Si–C bond, SiC fibers demonstrate a high mechanical resistivity and an excellent chemical stability. They also withstand against oxidation, at temperatures higher than 1500 °C. Zirconium carbide (ZrC) fibers [77, 78], Zr-doped SiC fibers [79, 80], SiOC fibers [81–84], SiCN fibers [85, 86] and Al-doped SiC fibers [87] are of other carbide ceramics which be formed as fibers. The introduction of heteroatoms, such as oxygen, nitrogen, zirconium, aluminum into SiC fibers improve their properties of ceramic fibers. For instance compared with

pure SiC fibers, Zr-doped SiC fibers exhibit a better oxidation resistance, even in high temperature.

Boron nitride (BN) has been widely used in fiber form [8, 88–90]. In terms of atomic arrangement and crystalline structure, BN is similar to carbon, as can form a hexagonal, cubic or tubular structure. Owing to these variable but strong structural atomic connections BN possesses a high thermal oxidation resistivity, low dielectric constant and high radiation absorption capacity. Moreover, BN exhibits a high thermal conductivity, a desired mechanical property and is electrically insulator, so can be widely used for structural, thermal, electrical, and optical applications. Silicon nitride (Si_3N_4) is another nitride ceramic compound which is widely applied in fiber preparation [91–93]. GaN fiber, as an important functional fiber, shows great application potential in semiconductor devices [94].

Other ceramic fibers such as ZnS nanofibers [95], boehmite nanofibers [96], hydroxyapatite fibers [97, 98], Cu_2ZnSnS_4 fibers [99, 100], etc are known for their excellent insulating or semi-conductor properties. The precursors and calcination conditions of various ceramic fibers are presented on Table 1. For preparation of ceramic fibers, usually a polymer is used as a support or fiber forming material. Poly(vinyl pyrrolidone) (PVP), poly(vinyl alcohol) (PVA), poly(ethylene oxide) (PEO), poly(vinyl butyral) (PVB) are the best candidate for this purpose. Oxide ceramic fibers are usually prepared by calcinating the precursor fibers in air, while carbide and nitride fibers are calcinated inert atmosphere. In general, it is necessary to select an appropriate processing method to process different ceramics into fibers depending on their chemical composition, resistivity, structure and physical properties.

Methods for Preparation of FCFs

Fabrication of FCFs is usually conducted by one of these typical methods; centrifugal spinning, electrospinning, solution blow spinning, self-assembly, chemical vapor deposition, atomic layer deposition, polymer conversion, etc.

Centrifugal Spinning

Centrifugal spinning employs the centrifugal force which is generated by a high-speed rotation, to convert a melt or a solution into fibers [101]. The schematic of a typical centrifugal spinning equipment, which is utilised for fiber preparation, is shown in Fig. 2a. Molten ceramic raw material is added in the spinning head, which is usually a metal container with multiple spinneret orifices evenly distributed around the sidewall of the spinning head. In order to keep the ceramic raw material in a molten state, the temperature of the spinning head is usually maintained at more than 1000 °C. The spinning head rotates at a very high speed and the rotating speed is usually higher than 2000 rpm [102]. When the centrifugal stress exceeds the surface tension of the ceramic melt, the ceramic melt will be injected from the spinneret orifices, forming bunch of ceramic melt jets. The molten ceramic flowing out of the sidewall is stretched by the centrifugal force and air frictional force, and reform into fine ceramic fibers with several centimeters length and overall diameter of 1 μm and higher.

In order to obtain FCFs with an average diameter of less than 1 um, the liquid (solution) spinning precursor is preferred precursors. This strategy is currently applied as the most popular methods in research and manufacturing (Fig. 2b) [69]. Various FCFs such as Al_2O_3 fibers [27, 28], SiO_2 fibers [18–20, 103], NiO fibers are typically fabricated by centrifugal spinning [55], Co_3O_4 fibers [55], $BaTiO_3$ fibers [60], TiO_2 fibers [42, 104], ZrO_2 fibers [33], ITO fibers [69, 105], SiC fibers [106], Si-doped TiO_2 fibers [43], SiOC fibers [107], α-Fe_2O_3 hollow fibers [108, 109], etc.

A crucial advantage of centrifugal spinning is its high throughput. The average production rate of a centrifugal spinning equipment with two nozzles is 50 g/h, which is two orders of magnitude higher than the lab-scale electrospinning apparatus [102]. More importantly, ceramic fibers with oriented structure can be obtained through rational design of configuration device (Fig. 2c, d) [18, 19]. Ceramic fibers can be oriented along the tangential direction in respect to the spinning head, while the centrifugal force is applied. As a result the ceramic fibers are formed with homogenous dimensions and desired mechanical property.

Electrospinning

Electrospinning is one of the most commonly used methods for fabrication of ceramic fibers [110–117]. Figure 3a shows the schematic of a typical electrospinning system consisted of a syringe, a metal nozzle, a power supply, and a conductive collector [117]. In electrospinning chamber, a high voltage electrical field is applied between the nozzle and the collector. When the electrostatic force is higher than the surface tension of the spinning solution, a liquid jet is formed at the nozzle. The electrified jet is stretched and whipped, and further split into multiple jets in an instable region (Fig. 3b, c) [118]. As the spinning solution moves to the collector, the solvent is evaporated, and the fiber diameter is reduced. Finally, the ultrafine fibers are obtained and wrapped around a rotating drum or on a flat collector, such as an aluminum paper or a metal sheet.

The typical steps in electrospinning of FCFs are explained as follows (Fig. 3d) [16]: (1) Preparation of a spinning solution containing polymers and ceramic precursors; (2) spinning the solution into ceramic precursor fibers by under electrical field; (3) calcination at high temperature in order

Table 1 Materials and calcination conditions for preparation of FCFs

Ceramic fibers	Precursors	Polymers	Solvents	Additives	Calcination conditions	References
SiO_2	TEOS	PVA	H_2O	H_3PO_4	5 °C min^{-1}, 600–1200 °C, in air	[1, 10–13, 16]
	TEOS	PVA	H_2O	Oxalic acid	5 °C min^{-1}, 800 °C for 2 h, in air	[15]
	TEOS	PVP	Ethanol	H_2O	6 °C min^{-1}, 550 °C for 1 h, in air	[17]
	TEOS	PVP	Ethanol	HCl, H_2O	850 °C, 6 h, in air	[18, 19]
	TEOS	PVP	Ethanol	HCl, H_2O	2 °C min^{-1}, 300, 600 and 900 °C, in air	[20]
	TEOS	/	Ethanol	HCl, H_2O	10 °C min^{-1}, 250–1000 °C for 3 h, in air	[14]
Al_2O_3	Aluminium acetate	PVP	Ethanol	Acetic acid	20 °C min^{-1}, 1000 °C for 2 h, in air	[21]
	Aluminum powder	PEO	H_2O	Formic acid, acetic acid	1 °C min^{-1}, 600 °C for 2 h, 5 °C min^{-1}, 700–1000 °C for 2 h, in air	[22]
	$Al(NO_3)_3{\cdot}9H_2O$, $AlCl_3{\cdot}6H_2O$, aluminum isopropoxide, aluminum powder	PEO	Nitric acid, H_2O	Pluronic P123	10 °C min^{-1}, 450 °C for 12 h/700–1100 °C for 0.5 h, in air	[24]
	$AlCl_3{\cdot}6H_2O$, aluminum powder	PVA	H_2O	Silica sol	4 °C min^{-1}, 600–1100 °C for 2 h, in air	[26]
	$AlCl_3{\cdot}6H_2O$, aluminum powder	/	H_2O	Silica sol	4 °C min^{-1}, 400–1200 °C for 4 h, in air	[27]
	$Al(NO_3)_3{\cdot}9H_2O$, aluminum isopropoxide	PVA, PVB, PVP	H_2O	/	5 °C min^{-1}, 900 °C for 1 h, in air	[25]
	Aluminum isopropoxide	PVA	H_2O	Nitric acid	3 °C min^{-1}, 650 °C/1200 °C for 3 h, in air	[28]

Table 1 (continued)

Ceramic fibers	Precursors	Polymers	Solvents	Additives	Calcination conditions	References
ZrO_2	$ZrOCl_2{\cdot}8H_2O$	/	H_2O	Hydrogen peroxide, $Y(NO_3)_3{\cdot}6H_2O$, acetic acid	1 °C min^{-1}, 800 °C for 1 h, 5 °C min^{-1}, 1200 °C for 1 h, in air	[29]
	Zirconium acetate	PVP	Acetic acid	/	200–1000 °C for 2 h, in air	[30]
	$ZrOCl_2{\cdot}8H_2O$	PVP	H_2O	$Y(NO_3)_3{\cdot}6H_2O$, citrate, acetate	600–1300 °C, in air	[31]
	Zirconium acetate hydroxide	PAN	DMF	$Y(NO_3)_3{\cdot}6H_2O$	5 °C min^{-1}, 280 °C for 1 h, 1 °C min^{-1}, 800 °C for 3 h, in air	[32]
	$ZrOCl_2{\cdot}8H_2O$	PVP	Ethanol, H_2O	/	2 °C min^{-1}, 800 °C for 200 min, in air	[2]
	$ZrOCl_2{\cdot}8H_2O$	/	H_2O_2, H_2O	$YCl_3{\cdot}6H_2O$	1.2–3 °C min^{-1}, 1300 °C for 3 h, in steam atmosphere	[33]
	Zirconium n-propoxide	PVP	Ethanol	$Y(NO_3)_3{\cdot}6H_2O$, fluorinated surfactant, acetylacetone	2 °C min^{-1}, 800 °C for 200 min, in air	[5]
TiO_2	Titanium (IV) isopropoxide	PVP	Ethanol, acetic acid	Zirconium acetate	2 °C min^{-1}, 600 °C for 1 h, in air	[34]
	Tetrabutyl titanate	PVP	Ethanol, acetic acid, H_2O	$Y(NO_3)_3{\cdot}6H_2O$	2 °C min^{-1}, 550 °C for 2 h, in N_2 atmosphere	[35]
	Titanium (IV) isopropoxide	PVP/PVAc/PLA	Ethanol, acetic acid, dimethyl carbonate	/	5 °C min^{-1}, 500–700 °C for 2 h, in air	[37]
	Titanium isopropoxide	PVP	Acetic acid, ethanol	Pluronic P123/F127	3–5 °C min^{-1}, 500–700 °C for 3 h, in air	[38]
	Titanium (IV) isopropoxide	PVC/PVP	THF, HCl/ethanol, acetic acid	/	600 °C/700 °C, in air	[39]
	Tetrabutyl titanate	PVP	Ethanol, acetic acid	/	2 °C min^{-1}, 450 °C for 200 min, in air	[2]
	$Ti(OiPr)_4$-isopropanol	PVA fiber template	/	/	600 °C, in air	[40]
	Titanium tetrachloride	Nanocellulose template	H_2O	/	450 °C for 8 h, in air	[41]
	Titanium tetrachloride, acetylacetone, triethylamine	/	H_2O, methanol, THF	TEOS	1.5 °C min^{-1}, 400–900 °C for 2 h, in steam atmosphere	[42]
	Titanium tetrabutoxide	/	H_2O, isopropyl alcohol, ethyl acetoacetate, THF	TEOS	500–900 °C, in steam atmosphere	[43]

Table 1 (continued)

Ceramic fibers	Precursors	Polymers	Solvents	Additives	Calcination conditions	References
ZnO	Zinc acetate dihydrate	PVP	DMF	/	400–600 °C for 2 h, in air	[44]
	$Zn(NO_3)_2{\cdot}6H_2O$	PVP	Ethanol, H_2O	$AgNO_3$	1 °C min^{-1}, 520 °C for 2 h, in air	[45]
	Zinc acetate	PVP	Ethanol	/	700 °C	[46]
	Zinc acetate	PVA	H_2O	$Ni(NO_3)_2$	650 °C for 3 h	[47]
	Zinc acetate dihydrate	PVC/PVP	THF, HCl/ ethanol, DMF	/	600 °C/700 °C	[39]
	$Zn(NO_3)_2$	PVP	H_2O, ethanol	/	6 °C min^{-1}, 550 °C for 1 h, in air	[17]
Mullite	Aluminum trisec-butoxide, polyhydromethylsiloxane	PVP	Isopropanol, DMF, ethyl-acetoacetate	/	2 °C min^{-1}, 800–1500 °C, in air	[48]
	Aluminium isopropoxide, $Al(NO_3)_3{\cdot}9H_2O$, TEOS	PVB	H_2O, ethanol	/	800–1400 °C for 2 h, in air	[49]
	Aluminum acetate, colloidal silica	PVP	H_2O, ethanol	Nitric acid, boric acid	5 °C min^{-1}, 800 °C for 1 h, 800–1200 °C for 1 h, in air	[50]
	Aluminum trisec-butoxide, polymethylsiloxane	PVP	Ethylacetoacetate, isopro-panol	/	2 °C min^{-1}, 800 °C for 2 h, in air	[51]
	Aluminum acetate, TEOS	PVP	H_2O, ethanol	Boric acid	5 °C min^{-1}, 800 °C for 1 h, 1000 °C for 1 h, in air	[52]
	TEOS, $Al(NO_3)_3{\cdot}9H_2O$	PVC	THF	/	600–1000 °C, in air	[53]
CeO_2	$Ce(acac)_3$	PVP	Ethanol, acetone	/	4.2 °C min^{-1}, 500 °C for 2 h, in air	[54]
Co_3O_4	$2CoCO_3{\cdot}3Co(OH)_2{\cdot}H_2O$	/	H_2O	Citric acid monohydrate	1 °C min^{-1}, 300–600 °C for 2 h, in air	[55]
NiO	$NiCO_3{\cdot}2Ni(OH)_2{\cdot}4H_2O$	/	H_2O	Citric acid monohydrate	1 °C min^{-1}, 300–600 °C for 2 h, in air	[55]
CuO	$Cu(NO_3)_2$	PVP	Ethanol, H_2O	/	6 °C min^{-1}, 500 °C for 1 h, in air	[17]
	Copper acetate	PVA	H_2O	/	10 °C min^{-1}, 500 °C for 4 h, in air	[56]
SnO_2	$SnCl_4{\cdot}5H_2O$	PVB	Ethanol	/	2 °C min^{-1}, 500 °C for 100 min, in air	[57]

Table 1 (continued)

Ceramic fibers	Precursors	Polymers	Solvents	Additives	Calcination conditions	References
$BaTiO_3$	Tetrabutyl titanate, barium acetate	PVP	Acetic acid, ethanol	/	2 °C min^{-1}, 750 °C for 1 h, in air	[2]
	Tetrabutyl titanate, barium acetate	PVP	H_2O, acetic acid, ethanol	/	2 °C min^{-1}, 400 °C for 3 h, 850 °C for 3 h, in air	[16]
	Tetrabutyl titanate, barium acetate	PVP	Ethanol, acetic acid, H_2O	/	2 °C min^{-1}, 550–1050 °C for 4 h, in air	[58]
	Tetrabutyl titanate, barium acetate	PVP	Ethanol, acetic acid	/	750 °C for 10 h, in air, oxygen, and nitrogen atmospheres	[59]
	Barium acetate, titanium isopropoxide	PVP	Acetic acid, ethanol	/	850 °C for 6 h, in air	[60]
$Li_{0.33}La_{0.56}TiO_3$	$C_{12}H_{28}O_4Ti$, $La(NO_3)_3{\cdot}6H_2O$, $LiNO_3$	PVP	H_2O, ethanol, acetic acid	/	2 °C min^{-1}, 400 °C for 4 h, 2 °C min^{-1}, 800 °C for 4 h, in air	[16]
	Tetrabutyl titanate, $La(NO_3)_3{\cdot}6H_2O$, $LiNO_3$	PVP	DMF, acetic acid	/	5 °C min^{-1}, 700–900 °C for 2 h, in air	[61]
	Titanium isopropoxide, $La(NO_3)_3{\cdot}6H_2O$, $LiNO_3$	PVP	DMF, acetic acid	/	/	[62]
$Li_7La_3Zr_2O_{12}$	$LiNO_3$, $La(NO_3)_3{\cdot}6H_2O$, zirconium acetate	PVP	H_2O, ethanol	/	2 °C min^{-1}, 400 °C for 4 h, 2 °C min^{-1}, 800 °C for 4 h, in air	[16]
$CaCu_3Ti_4O_{12}$	Tetra-n-butyl orthotitanate, copper(II) nitrate trihydrate, calcium nitrate tetrahydrate	PVP	Acetic acid, methanol, ethanol	/	10 °C min^{-1}, 600–900 °C for 4 h, in air	[63]
	Cupric acetate, calcium nitrate, tetrabutyl titanate	PVP	Acetic acid, ethanol	/	10 °C min^{-1}, 600–1130 °C, in air	[64]
	Tetra-n-butyl orthotitanate, copper(II) nitrate trihydrate, copper(II) chloride, calcium nitrate tetrahydrate, calcium chloride	PVP	Acetic acid, methanol, ethanol	/	900 °C for 4 h, in air	[65]
Yttrium–aluminum-garnet (YAG)	$AlCl_3{\cdot}6H_2O$, aluminum powder, yttrium acetate hydrate	/	H_2O	/	700–1000 °C for 2 h, in air	[67]
Indium tin oxide	$In(NO_3)_3{\cdot}4.5H_2O$, $SnCl_4{\cdot}5H_2O$	PVB	Ethanol	/	2 °C min^{-1}, 450 °C for 2 h in air, 2 °C min^{-1}, 300 °C for 1.5 h in H_2 atmosphere	[68]
	$In(NO_3)_3{\cdot}4.5H_2O$, $SnCl_4{\cdot}5H_2O$	PVP	H_2O	/	800 °C for 2 h, in air	[69]

Table 1 (continued)

Ceramic fibers	Precursors	Polymers	Solvents	Additives	Calcination conditions	References
YBCO	Yttrium acetate hydrate, barium acetate, copper acetate monohydrate	PVP	Methanol, acetic acid, propionic acid	/	1 °C min^{-1}, 450 °C, 3 h/3 °C min^{-1}, 820 °C, 14 h/1 °C min^{-1}, 925 °C, 1 h/1 °C min^{-1}, 725 °C, 3 h/3 °C min^{-1}, 450 °C, 12 h, in O_2 atmosphere	[70]
MFe_2O_4 (M = Cu, Co, Ni)	$Fe(NO_3)_3{\cdot}9H_2O$, $Cu(NO_3)_2{\cdot}3H_2O$, $Co(NO_3)_2{\cdot}6H_2O$, $Ni(NO_3)_2{\cdot}6H_2O$	PVP	Ethanol, DMF, glacial acetic acid	/	5 °C min^{-1}, 200 °C for 2 h, 2 °C min^{-1}, 800 °C for 2 h, in air	[71]
SiC	Methyltrimethoxysilane, dimethyldimethoxysilane	/	Ethanol	H_2O, nitric acid	/	[6]
	PCS	PVP	DMF, THF	/	2 °C min^{-1}, stabilized at 210 °C for 2 h in air, calcinated at 800 °C for 2 h, 1300 °C for 2 h in Ar	[72]
	PCS	PMMA	Toluene, DMF	/	Stabilized at 170 °C for 3 h in air, calcinated at 1100–1500 °C in N_2/calcinated at 1500 °C in Ar	[73]
	Methyltrimethoxysilane, dimethyldimethoxysilane	/	Ethanol, H_2O	/	5 °C min^{-1}, 1550 °C for 2 h, in Ar	[75]
	PCS	PEO	Xylene, H_2O	Sodium dodecyl sulfate	Stabilized at 200 °C for 10 h in air, calcinated at 1400 °C for 2 h in Ar	[76]
	Polysilocarbonsilane	/	/	Aluminium acetylacetonate	Stabilized at 160–220 °C for 6–8 h in air, calcinated at 1800 °C in Ar	[87]
SiOC	PCS	PS	Xylene, DMF	Sodium dodecyl sulfate	1 °C min^{-1}, stabilized at 210 °C for 2 h in air, calcinated at 1100 °C in Ar	[81]
	Silicone resin	PVP	Isopropanol, DMF, chloroform	Dibutyltin dilaurate, Zr-acetylacetonate, Triton X-100 surfactant, sodium chloride	Stabilized at 200 °C for 1 h in air, 2 °C min^{-1}, calcinated at 1000 °C for 2 h in Ar	[82–84]
SiCN	PCS	PVP	DMF, chloroform	/	2 °C min^{-1}, 180 °C, 1 °C min^{-1}, 210 °C for 2 h; 2 °C min^{-1}, 250 °C, 1 °C min^{-1}, 850 °C, 2 °C min^{-1}, 1300 °C for 3–7 h in N_2	[85]

Table 1 (continued)

Ceramic fibers	Precursors	Polymers	Solvents	Additives	Calcination conditions	References
ZrC	$ZrOCl_2 \cdot 8H_2O$, PAN, sucrose	/	DMF	/	3 °C min^{-1}, 1200–1400 °C for 2 h in Ar	[77]
	Zirconium acetyl acetonate, phenolic resin	2,4-pentanedione, ethanol	H_2O, H_2SO_4	/	800–1600 °C for 2 h in Ar	[78]
BN	Boric acid, melamine	/	H_2O, tertiary butyl alcohol	/	1200 °C for 3 h in NH_3	[88]
Si_3N_4	Methyltrimethoxysilane, dimethyldimethoxysilane	/	Ethanol	H_2O, nitric acid	5 °C min^{-1}, 1500 °C for 2 h in N_2	[91]
	Silica sol, carbon black	/	/	Cetyltrimethylammonium bromide	3 °C min^{-1}, 1600 °C for 3 h in N_2	[93]
GaN	Gallium nitrate	PVP	H_2O, ethanol	/	10 °C min^{-1}, 500 °C for 4 h in air, 450 °C for 1 h in air, 2 °C min^{-1} (NH_3), 850 °C for 2 h in Ar	[94]
ZnS	Zinc acetate	PVP	Ethanol, H_2O	/	2 °C min^{-1}, 550 °C for 1 h in air, 500 °C in H_2S atmosphere	[95]
Boehmite	Boehmite, aluminum hydroxide, hexamethylenetetramine	/	Acetic acid	/	600–1300 °C	[96]
Hydroxyapatite	NaOH, $CaCl_2$, $NaH_2PO_4 \cdot 2H_2O$	/	H_2O, methanol, oleic acid	/	/	[97]
	$CaCl_2$, sodium oleate, $(NaPO_3)_6$	/	H_2O	/	/	[98]
Cu_2ZnSnS_4	$CuCl_2$, $ZnCl_2$, $SnCl_4 \cdot 5H_2O$, thiourea	PVP, cellulose acetate	Acetone, H_2O, ethanol	/	2 °C min^{-1}, 450 °C for 3 h in N_2	[99]
	$Cu(CH_3COO)_2$, $Zn(CH_3COO)_2$, $SnCl_2$, thiourea	PVB	Ethanol	/	0.5 °C min^{-1}, 150–550 °C, in air	[100]

TEOS tetraethyl orthosilicate, *PVA* poly(vinyl alcohol), *PVP* poly(vinyl pyrrolidone), *PEO* poly(ethylene oxide), *PVB* poly(vinyl butyral), *DMF N,N*-dimethylformamide, *PVAc* poly(vinyl acetate), *PLA* poly(lactic acid), *THF* tetrahydrofuran, *PVC* poly(vinyl chloride), *PCS* polycarbosilane, *PMMA* poly(methyl methacrylate), *PS* polystyrene, *PAN* polyacrylonitrile, *BN* boron nitride

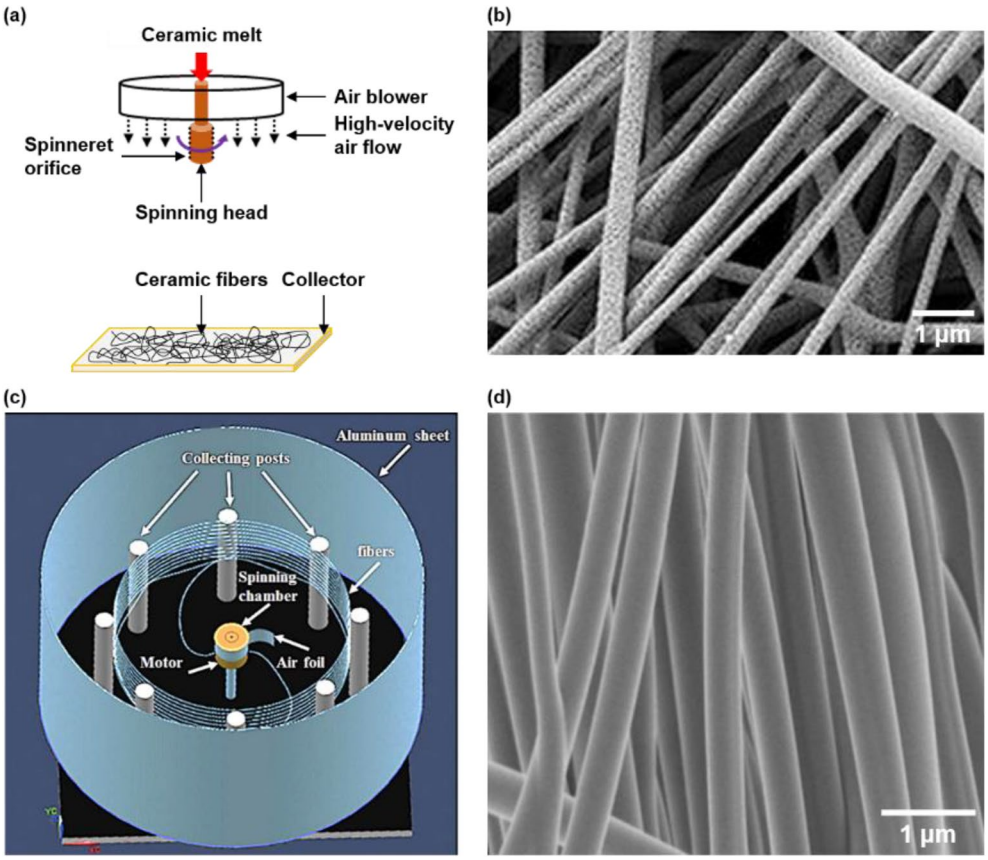

Fig. 2 Fabrication of FCFs with centrifugal spinning. **a** Schematic of a typical centrifugal spinning equipment. **b** SEM image of ITO nanofibers with disordered distribution. **c** Schematic of another typical centrifugal spinning equipment with different configuration. **d** SEM image of aligned SiO_2 nanotube fibers. **b** Reproduced with permission from Ref. [69]. Copyright 2015, Springer Nature BV. **c** Reproduced with permission from Ref. [19]. Copyright 2014, Elsevier. **d** Reproduced with permission from Ref. [18]. Copyright 2014, Elsevier

to eliminate the organic components and residuals electrospun. Moreover, ceramic precursor sols can be used to directly produce FCFs by electrospinning without additional polymers [119, 120]. A polymer-free electrospinning significantly reduces the volume shrinkage of the ceramic fibers during calcination and cuts the production cost.

The main advantages of electrospinning is that the structure and morphology of the FCFs can be easily controlled by tuning the composition of the precursor solution, or alternation of spinning and calcination conditions. So far, electrospinning of FCFs has mostly remained in the research level, which can be basically because of the low rate of production and hard process and parameters controlling in a potential high scale pilot.

Solution Blow Spinning

Solution blow spinning is an economical and effective fiber preparation technology, which can produce a variety of fiber materials with high efficiency and low cost, including ceramic fibers, metal fibers and polymer fibers [3, 4, 121–125]. Figure 4a is a schematic diagram of a typical solution blow spinning device, which consists of a compressed air source, a collector and a solution conveying device. Solution blow spinning device contains a pair of coaxial nozzles. The spinning solution is extruded through the inner nozzle, and the high-speed gas flow is ejected through the outer nozzle (Fig. 4b). The spinning solution forms a jet under the shear action of the high-speed gas flow. The jet is further split, drawn and refined, and the solvent is volatilized in the process of jet movement (Fig. 4c, d). Finally, the fibers are formed, solidified, and collected on the collector.

The process of FCFs fabrication by solution blow spinning is partly similar to electrospinning, as it starts with preparation of spinning solution, which contains a polymer phase and a ceramic disperse or particles phase. The polymer-ceramic precursor solution then forms the composite fibers by being subjected to blow spinning and finally calcination in high temperature is applied to form the ceramic

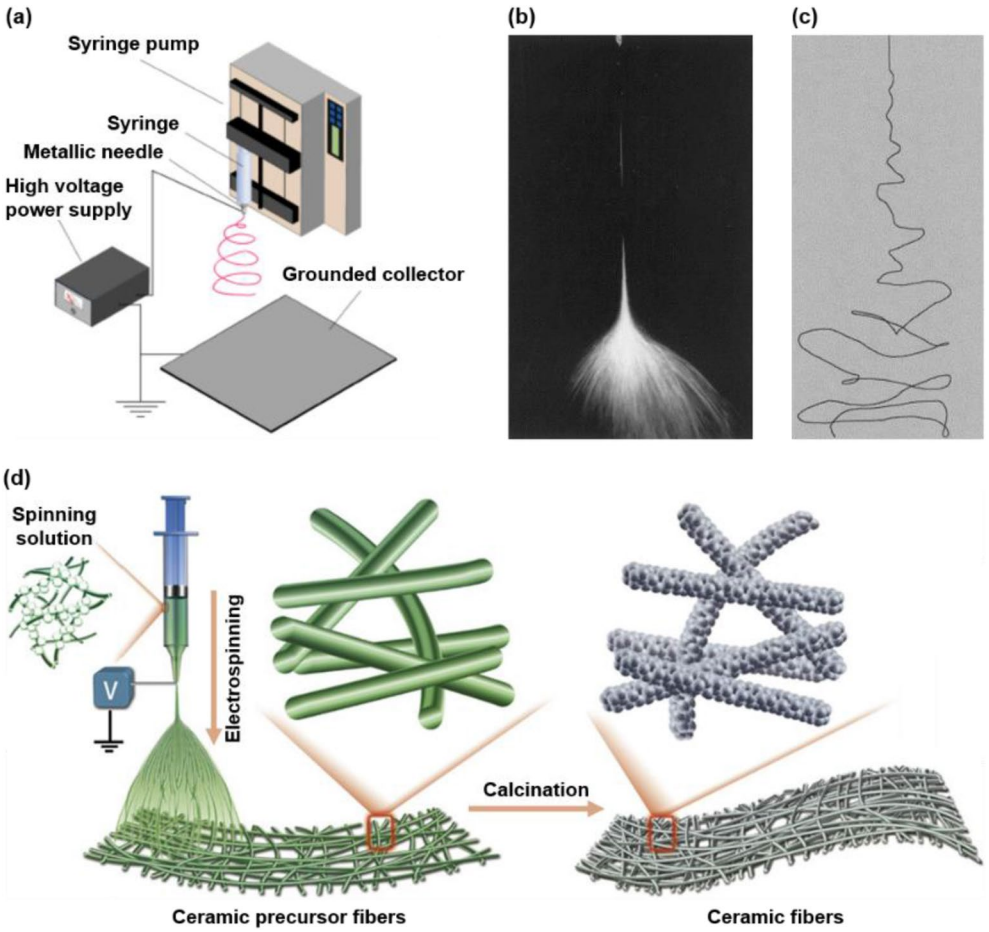

Fig. 3 Electrospinning for preparation of FCFs. **a** Schematic of a typical electrospinning device. **b** Digital image showing the electrified spinning solution jet. The exposure time is 1/250 s. **c** Digital image shows the trace of the electrified spinning solution jet in the instable region. The exposure time is 18 ns. **d** Procedures for the preparation of FCFs by electrospinning. **a** Reproduced with permission from Ref. [117]. Copyright 2006, John Wiley and Sons. **b**, **c** Reproduced with permission from Ref. [118]. Copyright 2001, Elsevier. **d** Reproduced with permission from Ref. [16]. Copyright 2019, Elsevier

fibers. Here we consider the preparation of SiO_2 fibers by solution blow spinning as an example. The PVA-TEOS solution is first prepared (Fig. 4e), and the PVA-SiO_2 composite microfibers are formed via blow spinning of the solution (Fig. 4f). Finally, the composite microfibers are processed into SiO_2 fibers, through calcination at high temperature (Fig. 4g). After removing the organic components and residual, the average diameter of the calcinated fibers decreases significantly.

Solution blow spinning is a simple procedure and spends less spinning solution compared with electrospinning. This is one of the reason that makes this method quite popular for the fabrication of FCFs [2–4, 39, 53, 57, 62, 68, 70, 71, 128]. The blow spinning equipment uses high-speed gas flow as the driving force, and does not need a high voltage electrostatic field, so it has a higher spinning efficiency. In addition, samples as the fibers can be collected by any type of collector, such as plastic or metal meshes or nonwoven fabrics. Also, unlike electrospinning, solution blow spinning can produce both two-dimensional films or webs (Fig. 4h), as well as three-dimensional sponges (Fig. 4i).

Self-assembly

Nanofibers can be prepared by binding the small molecules together through intermolecular interactions. This chemical process is generally known as self-assembly. Nanofibers can be assembled by different mechanisms depending on the chemical structure of their unit small molecules. A common mechanism for nanofibers assembly, is the formation of hydrogels, which consist of two mutually permeating phases, namely liquid phase (water is the most common) and solid phase (a network of nanofibers formed by self-assembly of hydrogel molecules). The dried nanofibers can be achieved by removing the liquid phase of the hydrogels.

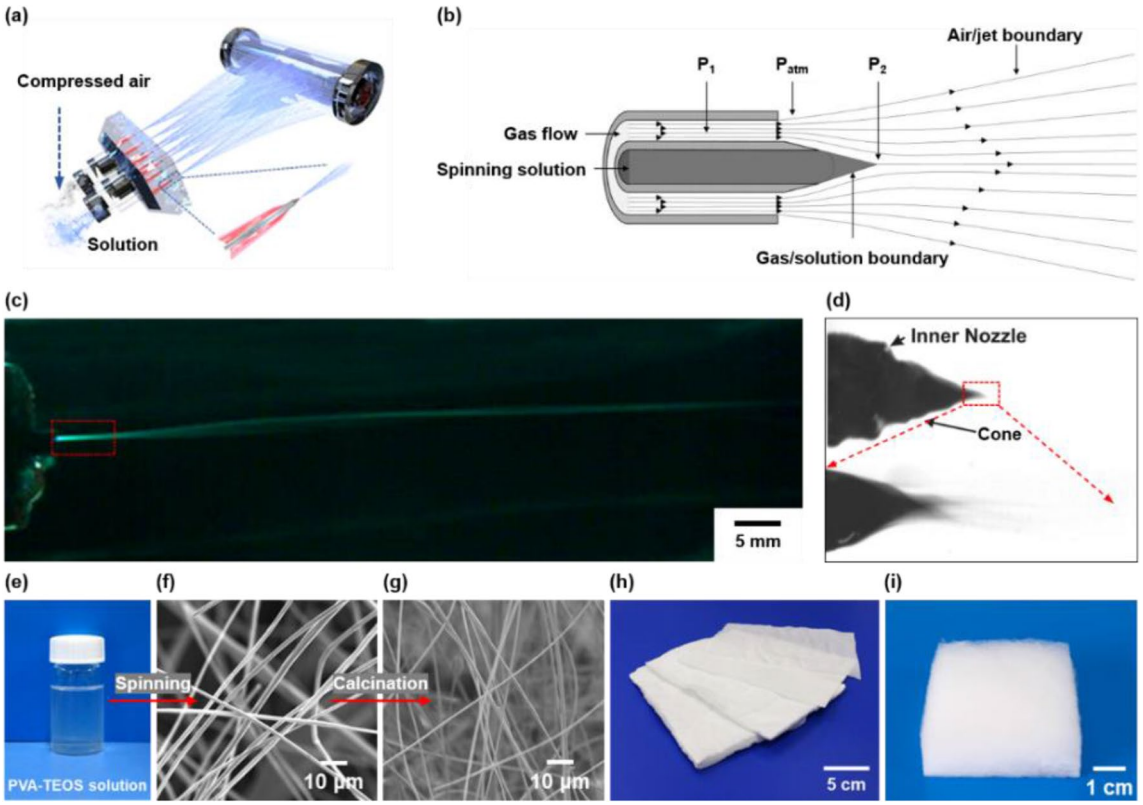

Fig. 4 Solution blow spinning for preparation of FCFs. **a** Schematic of a solution blow spinning device. **b** Schematic showing the state of the nozzle position, where the spinning solution is pumped through the inner nozzle and stretched by the high-pressure gas flow (P_1) from the outer nozzle. An area of low pressure (P_2) is formed around the inner nozzle, which draws the spinning solution into a cone. **c** Digital image of the spinning solution jet taken by a high-speed camera. **d** Digital image showing the Taylor cone of spinning solution formed at the end of the spinneret. **e** Digital image of the PVA-TEOS solution. **f** SEM image of the PVA-SiO_2 composite microfibers. **g** SEM images of the SiO_2 microfibers. **h** Digital image of ceramic fiber papers. **i** Digital image of a ceramic fiber sponge. **a**, **h** Reproduced with permission from Ref. [4]. Copyright 2020, American Chemical Society. **b**, **d** Reproduced with permission from Ref. [126]. Copyright 2009, John Wiley and Sons. **c** Reproduced with permission from Ref. [127]. Copyright 2014, American Chemical Society. **e**–**g**, **i** Reproduced with permission from Ref. [3]. Copyright 2020, Springer Nature

Li et al. [88] prepared BN nanoribbon aerogels using hydrogen bond self-assembly method (Fig. 5). The preparation of BN nanoribbon aerogels requires four serial steps (Fig. 5a): (1) Boric acid (B) and melamine (M) are mixed in a hot distilled water/tertiary butanol (TBA) co-solvent; (2) The mixed solution is cooled to room temperature (25 °C) by ultrasonic treatment to obtain M·2B hydrogel; (3) M·2B hydrogel is freeze-dried to obtain aerogel-like M·2B precursor; (4) After pyrolysis of M·2B in an ammonia atmosphere at 1200 °C for 3 h, lightweight, thermal insulating and hydrophobic BN nanoribbon aerogel are finally obtained. The BN nanoribbons with high aspect ratio are intertwined with each other to form an aerogel network structure (Fig. 5b). In addition, these BN nanoribbons are able to withstand deformation due to stresses, such as bending and twisting, showing excellent flexibility (Fig. 5c).

Atomic Layer Deposition

Atomic layer deposition (ALD) is a method for producing thin films by deposition of solid phase from a vapor precursor, on the surface of a deposition matrics. Tubular ceramic materials have been prepared by ALD [41, 129, 130]. Since the atoms are deposited layer by layer, the resultant materials forms a homogenous structure and a controllable thickness. Xu et al. [130] prepared Al_2O_3 fiber sponges with hollow fibrous structure by ALD (Fig. 6a). Polyvinyl propylene (PVP) fiber sponges were first prepared by solution blow spinning technique (Fig. 6b), and then a layer of Al_2O_3 was coated on the surface of the PVP fibers using ALD (Fig. 6c), and finally the PVP fiber scaffold was removed by calcination, and a high resilience Al_2O_3 fiber sponges with an ultralow density and thermal conductivity remained (Fig. 6d).

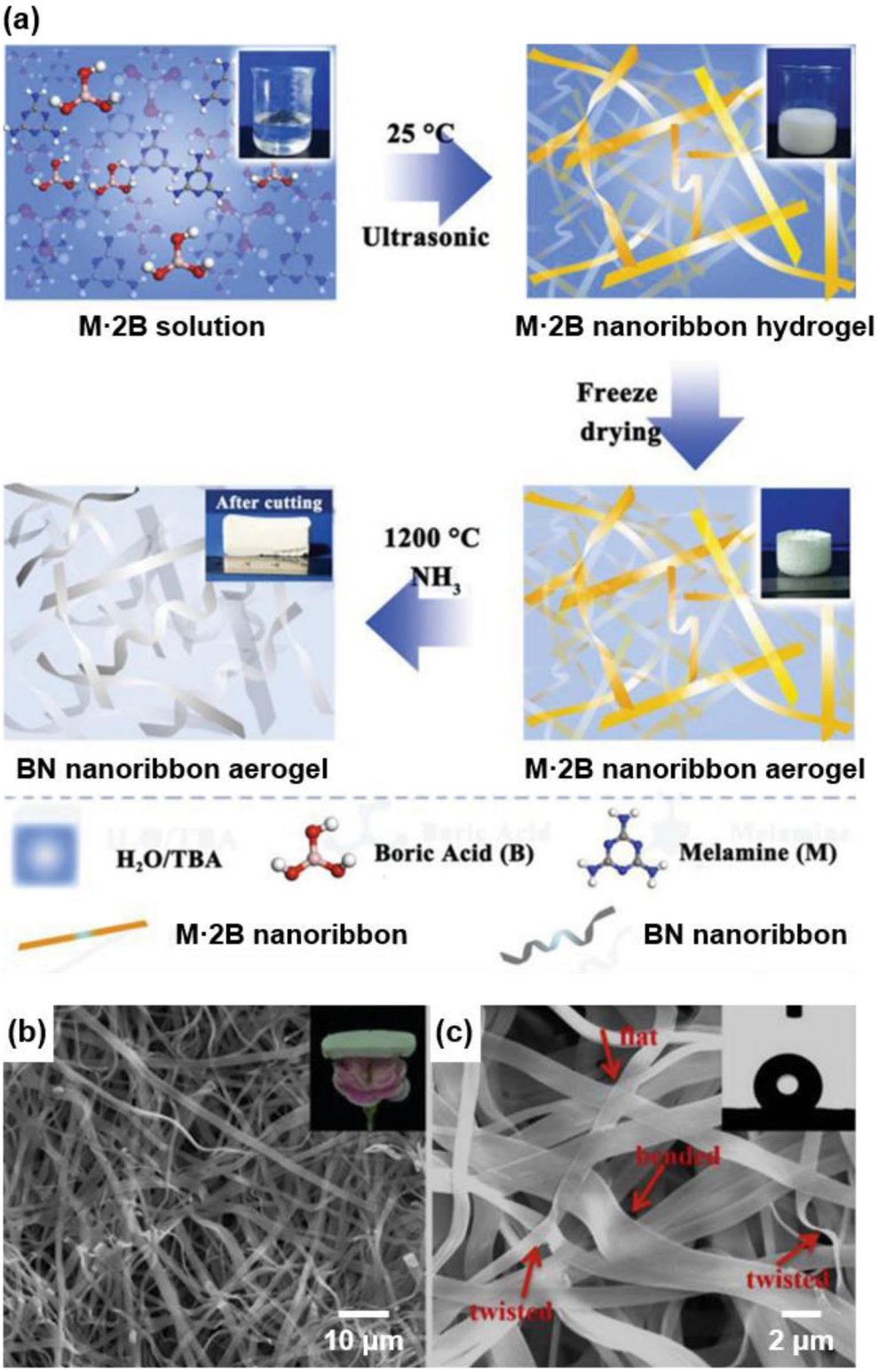

Fig. 5 Preparation of BN nanoribbons by hydrogen bond self-assembly. **a** Schematic showing the synthesis of BN nanoribbons. **b**, **c** SEM images of the BN nanoribbons. Reproduced with permission from Ref. [88]. Copyright 2019, John Wiley and Sons

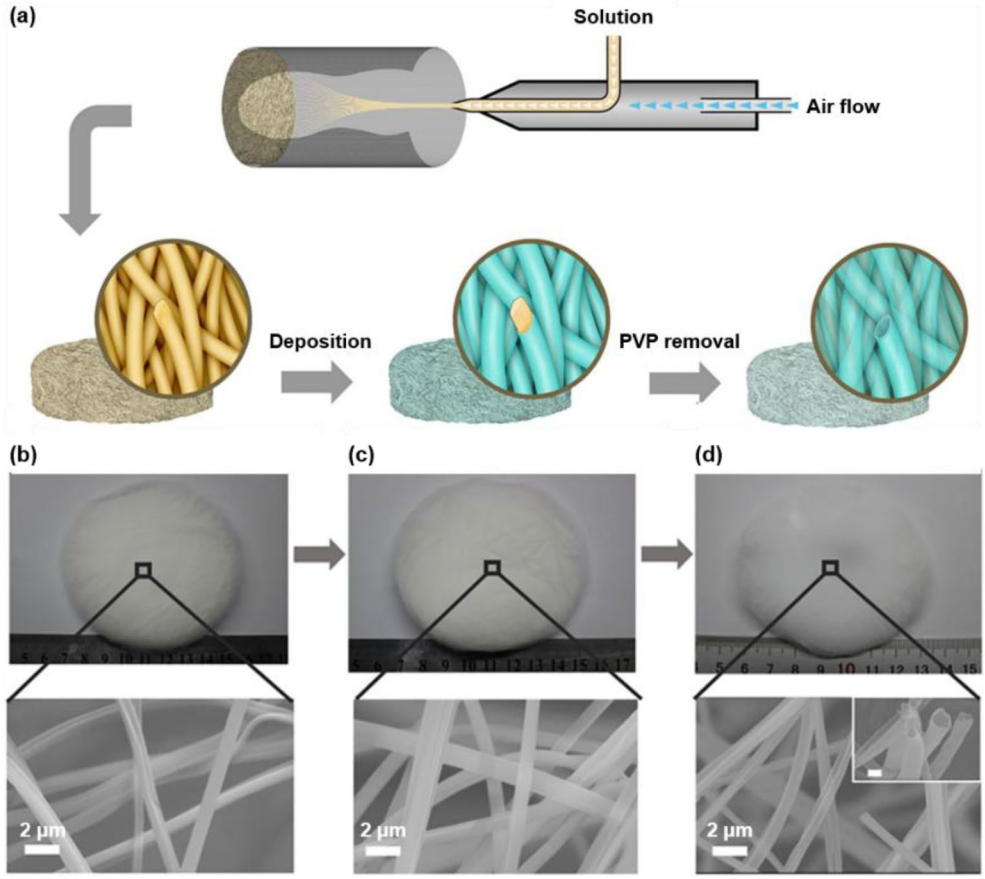

Fig. 6 Preparation of Al_2O_3 fiber sponges by ALD. **a** Schematic showing the preparation of Al_2O_3 fiber sponges by ALD method. The preparation process includes preparation of PVP fiber sponge by solution blow spinning, atomic layer deposition of Al_2O_3 layer, and PVP removal by calcination. Digital images and SEM images of **b** PVP fiber sponges prepared by solution blow spinning, **c** PVP-Al_2O_3 composite fiber sponges obtained by atomic layer deposition of Al_2O_3 layer, and **d** Al_2O_3 fiber sponges obtained after template removal. Reproduced with permission from Ref. [130]. Copyright 2017, John Wiley and Sons

In addition to synthetic fibers, natural fibers have also been used as template to prepare FCFs using the ALD process. Korhonen et al. [41] prepared ZnO, TiO_2 and Al_2O_3 nanotube aerogels by ALD, where nanocellulose were employed as the scaffold fibers.

Chemical Vapor Deposition

Chemical vapor deposition (CVD) is used for preparation of uniform layers (films) from inorganic precursors. This process occurs together with chemical reactions between ingredients in vapor phase, leaving a uniform solid layer. In recent years, CVD method has been frequently used for preparation of carbide and nitride FCFs, such as SiC fibers, Si_3N_4 fibers, etc. [6–8, 91, 131, 132].

Su et al. [6] prepared highly porous three-dimensional SiC nanowire aerogels by CVD (Fig. 7). The process in general requires three sequential steps: (1) Initial materials are nucleated and grown on the graphite substrate; (2) raw materials are nucleated and grown on the surface of the existing nanowires layer by layer; (3) highly porous three-dimensional SiC nanowire aerogels are detached from the graphite substrate (Fig. 7a). The SiC nanowire aerogels obtained in this work has an ultralow density of 5 mg cm^{-3} (Fig. 7b, c), and a diameter of 20–50 nm and a length of tens to hundreds micrometers (Fig. 7d, e). Such tiny ceramic fibers are practically hard to be prepared by bow spinning or electrospinning.

Polymer Conversion

Polymer conversion is a method for preparing high temperature resistant FCFs from polymers containing silicon (Si), carbon (C), nitrogen (N) and other elements [133]. The polymer precursors are first processed into fibrous materials by fiber processing methods, such as electrospinning, solution

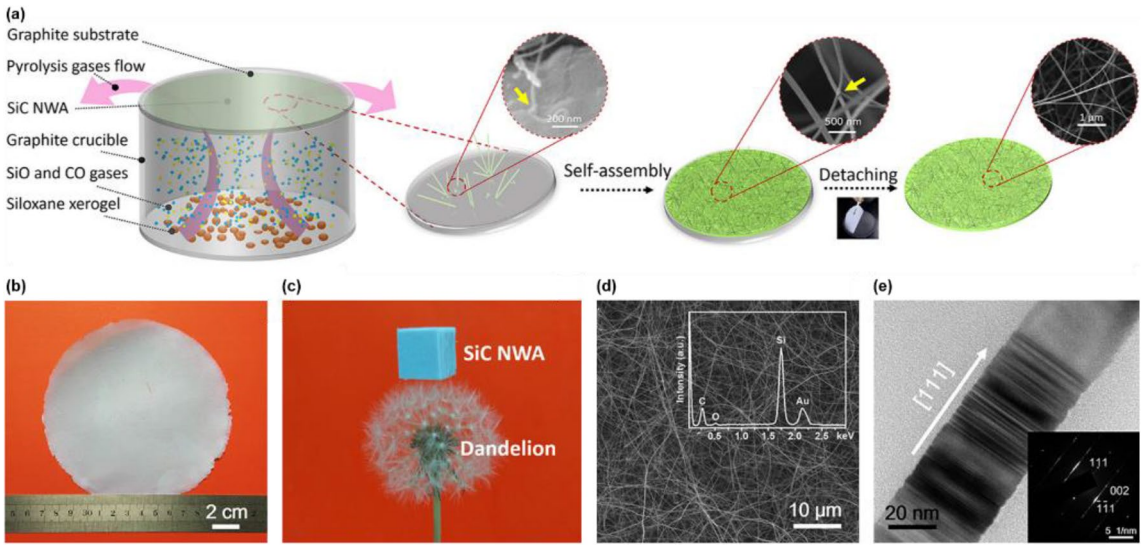

Fig. 7 Preparation of SiC nanowire aerogels by CVD method. **a** Schematic showing the preparation of SiC nanowire aerogels by CVD method. **b** Digital image of a piece of SiC nanowire aerogel. **c** Digital image of a SiC nanowire aerogel standing on a dandelion. **d** SEM image of the SiC nanowire aerogels showing the highly porous three-dimensional structure. **e** TEM image of the SiC nanowires. Reproduced with permission from Ref. [6]. Copyright 2018, American Chemical Society

blow spinning. Then the polymer fibers are subjected to thermal curing. During thermal treatment polymer chains are cross-linked and transformed from hot melt polymers to thermosetting polymers. Finally, a high temperature calcination eliminates the organic components and residuals, forms the FCFs.

Polymer conversion method is often used to prepare non-oxide ceramic fiber materials, and SiC fiber is the most studied [72, 73, 76, 134–140]. Hou et al. [134–137, 139] developed SiC fibers and a series of modified SiC fibers by electrospinning combined with polymer precursor conversion: First, the spinning solutions containing polymers, ceramic precursors and other ingredients such as modifiers are prepared, then the composite fibers are prepared by electrospinning process, and eventually the SiC fibers or modified SiC fibers are obtained by thermal curing and pyrolysis (Fig. 8).

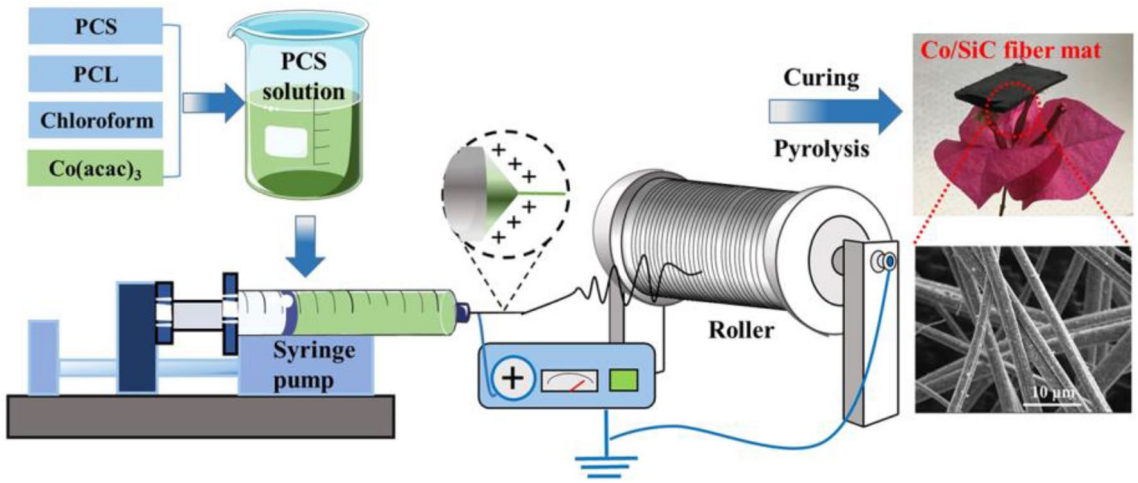

Fig. 8 Preparation of Co/SiC fiber mats by electrospinning combined with polymer precursor conversion method. The photograph on the top right corner, shows the Co/SiC fiber mat, and the SEM image, shown at bottom right corner, shows the morphology of the Co/SiC fiber mat, prepared by polymer conversion. Reproduced with permission from Ref. [134]. Copyright 2020, American Chemical Society

Table 2 Comparison of different FCF preparation methods

Methods	Material types	Advantages	Disadvantages	Fiber diameter	Industrialization prospect	References
Centrifugal spinning	Melt	High efficiency	Relatively poor flexibility	> 1 μm	High	[102]
	Solution	High efficiency; broad material choice	Removal of polymer	Tens of nanometers to a few microns	Relatively high	[20, 28, 60, 69, 104]
	Sol	High efficiency; high yield; polymer free	Ununiform diameter	Hundreds of nanometers to tens of microns	Relatively high	[27, 42, 43, 55]
Electrospinning	Solution	Small and uniform diameter; diverse compositions and morphologies	Low efficiency; high voltage; removal of polymer	Tens of nanometers to a few microns	Relatively low	[110, 112–114, 116]
	Sol	High yield; polymer free	Nonuniform diameter; high voltage	Tens of nanometers to a few microns	Relatively low	[14, 120, 145–147]
Solution blow spinning	Solution	Simple and safe process; high efficiency; diverse compositions and structures	Removal of polymers	Tens of nanometers to a few microns	Relatively high	[2–4, 39, 53, 62, 68, 70, 71, 123, 128]
Self-assembly	Solution	Ribbon structure	Limited material choice; low efficiency; removal of organic	Width: hundreds of nanometers to a few microns Thickness: a few nanometers	Low	[88]
Atomic layer deposition	Solution	Hollow structure; controllable diameter	Complicated process; low efficiency; limited material choice	Tens of nanometers to a few microns	Low	[41, 129, 130]
Chemical vapor deposition	Gas	Small and uniform diameter; non-oxide component	Low efficiency; limited material choice	Tens to hundreds of nanometers	Low	[6–8, 91, 131, 132]
Polymer conversion	Solution	Non-oxide component	Low efficiency; calcination in inert atmosphere	Tens of nanometers to a few microns	Relatively low	[72, 73, 76, 134–140]

Comparison of Different FCF Preparation Methods

Based on the above discussions, we can see that different FCF preparation methods are associated with advantages and disadvantages. The structure and properties of different ceramic fibers are summarized in Table 2. Out of the above-mentioned methods, only centrifugal spinning is suitable for processing the ceramic melts [102]. Preparation of ceramic fibers by centrifugal spinning, from a melt precursor is an efficient approach, but highly energy consuming. However, electrospinning necessarily works with a colloidal and polymeric solution as a precursor [117, 120]. So far various polymeric fibers have been prepared by melt electrospinning [141, 142], but it is still hard to fabricate the ceramic fibers by melt electrospinning.

Ceramic fiber materials with different structures and morphologies can be obtained from different preparation methods. Hollow ceramic fibers can be obtained by electrospinning [143] and ALD method [130]. Ribbon structural ceramic fiber materials can be prepared by self-assembly method [88]. Centrifugal spinning and electrospinning can be used to fabricate FCFs with aligned structure [18, 144]. Compared with other methods, the FCFs produced by CVD method exhibit smaller and more uniform diameter [6]. Non-oxide ceramic fibers are usually prepared by chemical vapor deposition and polymer conversion [6, 74].

In terms of material choices, centrifugal spinning, electrospinning and solution blow spinning can be used to prepare various ceramic fiber materials. However, the material choices for other ceramic fiber preparation methods, including self-assembly, ALD, CVD, and polymer conversion, are limited. For example, the self-assembly method can only use small molecules to assemble and form supramolecular hydrogels through weak interactions to prepare fiber materials, especially for the preparation of ceramic fiber materials, the choice of raw materials is very limited.

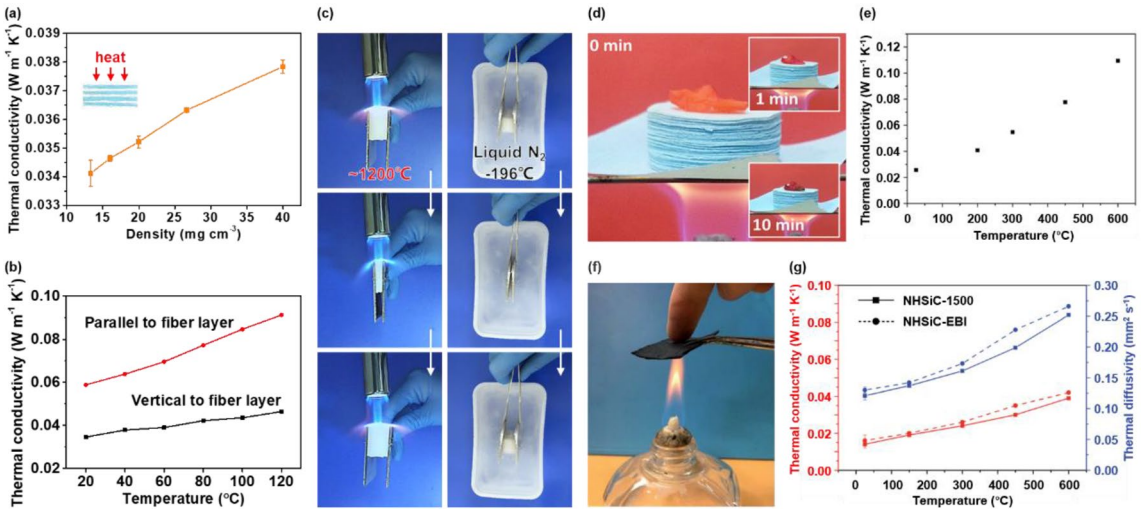

Fig. 9 Thermal insulation properties of FCFs. Thermal conductivity of SiO_2-Al_2O_3 composite fiber sponges **a** with different densities, **b** along two different layer directions at different temperatures. **c** Digital images showing the compressibility of the SiO_2-Al_2O_3 composite fiber sponges burned with a butane blowlamp and immersed in liquid nitrogen, respectively. **d** Digital image showing the SiC nanowire aerogels with a thickness of 10 mm can protect fresh petals from withering when heated by an alcohol lamp. **e** Thermal conductivity of the SiC nanowire aerogels at different temperatures in a nitrogen atmosphere. **f** Digital image showing the thermal insulation performance of SiC fiber mat. **g** Thermal conductivity and thermal diffusivity of SiC fiber mat at different temperatures. **a**–**c** Reproduced with permission from Ref. [3]. Copyright 2020, Springer Nature. **d**–**e** Reproduced with permission from Ref. [6]. Copyright 2018, American Chemical Society. **f**, **g** Reproduced with permission from Ref. [73]. Copyright 2017, Royal Society of Chemistry

From the perspective of production efficiency of ceramic fibers, centrifugal spinning has higher spinning efficiency and industrial application prospect, especially centrifugal melting spinning. In addition to centrifugal spinning, compared with other ceramic fibers, solution blow spinning has attracted more and more attention in recent years for its higher efficiency and better fiber material properties, showing a broad prospect of industrial application [123].

Applications of FCFs

Thermal Insulation

Because ceramic fiber materials have the advantages of low density, high temperature resistance, low thermal conductivity, and good chemical stability, they are particularly suitable for thermal insulation purposes, especially for aerospace and other fields that need lightweight thermal insulation materials. Ceramic fiber materials are composed of solid fibers and air between the fibers, in which the solid fibers are a skeleton and endow the material with a specific shape. The thermal insulation property of ceramic fiber materials is mainly attributed to the air component between the solid fibers. In addition, the ceramic fiber materials usually have excellent flexibility, which makes it better than ordinary bulk insulation materials. Therefore, application of ceramic fibers material, as high temperature insulation materials, has attracted increasing attention in recent years [1, 2, 6, 10, 73, 91, 148–150].

We prepared SiO_2-Al_2O_3 composite fiber sponges with anisotropic lamellar structure and low density [3]. Due to the low density and layered structure, the sponges with a density of 13 mg cm^{-3} have a low thermal conductivity of 0.034 W m^{-1} K^{-1} perpendicular to the fiber layer direction at 20 °C. The higher the density of the sponges, the higher the thermal conductivity (Fig. 9a). The anisotropic structure endows the sponges with anisotropic thermal properties, and the thermal conductivity parallel to the fiber web is significantly higher than that perpendicular to the fiber layer. In addition, the sponges along the two different fiber layers have greater thermal conductivity at higher temperatures (Fig. 9b). It should be emphasized that the sponges are able to withstand high temperature of around 1200 °C and liquid nitrogen temperature of − 196 °C, and maintain excellent compression resilience under these temperature conditions (Fig. 9c).

Su et al. [6] prepared three-dimensional SiC nanowire aerogels by CVD method. The aerogels demonstrated excellent thermal insulation property, as a 10 mm-thick SiC nanowire aerogels can protect fresh petals from withering, when it is heated by an alcohol lamp in 10 min (Fig. 9d). In a nitrogen atmosphere, the thermal conductivity of the SiC nanowire aerogels at room temperature is only 0.026 W m^{-1} K^{-1}. With the increase of temperature, the thermal conductivity of the SiC nanowire aerogels gradually

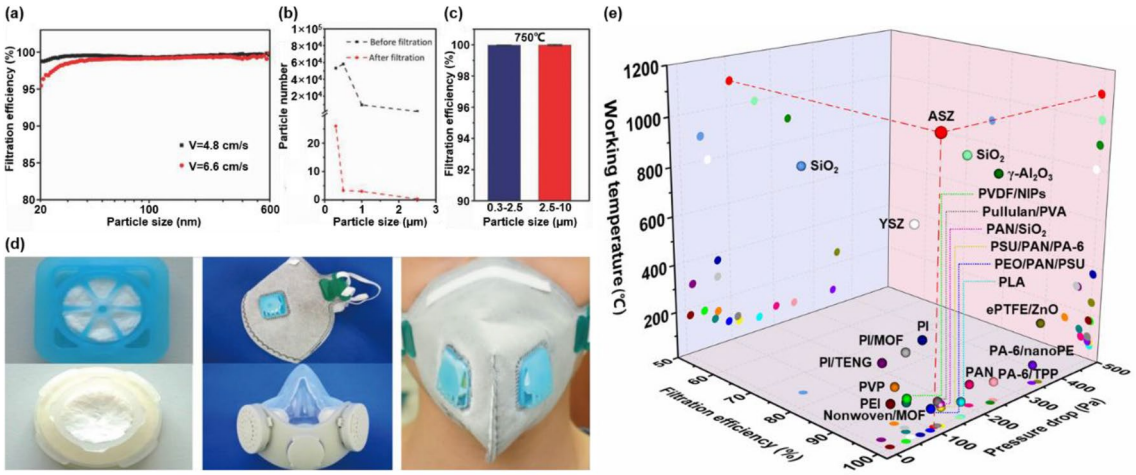

Fig. 10 Air filtration application of FCFs. **a** Filtration efficiency of YSZ nanofiber sponges to NaCl particles with different particle sizes at different airflow velocities at room temperature. **b** PM concentration before and after filtration with YSZ sponges at 750 °C. **c** Filtration efficiency of YSZ sponges to $PM_{0.3–2.5}$ and $PM_{2.5–10}$ at 750 °C. **d** Digital images showing the application of hydroxyapatite nanowire aerogels in breathing masks. **e** Comparison of filtration properties and working temperature for the ASZ papers and other flexible filter materials. **a**–**c** Reproduced with permission from Ref. [5]. Copyright 2018, John Wiley and Sons. **d** Reproduced with permission from Ref. [98]. Copyright 2018, American Chemical Society. **e** Reproduced with permission from Ref. [4]. Copyright 2020, American Chemical Society

increases due to the increasing gas thermal radiation, at high temperatures (Fig. 9e). Liu et al. [73] prepared nitrogen-doped hollow SiC fiber mats by electrospinning method combined with polymer precursor conversion method. The hollow SiC fiber mats have good thermal insulation property (Fig. 9f), and the thermal conductivity at 600 °C is only 0.039 W m^{-1} K^{-1} (Fig. 9g).

In order to achieve good thermal insulation property of ceramic fiber materials, one of the most important factors is having the low density ceramic fibers. In general, the lower the density, the lower the thermal conductivity. For instance, an ultralow density of approximately 0.2 mg cm^{-3} has been achieved for SiO_2 nanofibrous aerogels, endowing them with an ultralow thermal conductivity of 23.27 mW m^{-1} K^{-1} [148]. The special structural design can effectively reduce the density of ceramic fiber materials, and thus decrease their thermal conductivity, such as lamellar ceramic fiber sponges obtained by solution blow spinning [3] and oriented ceramic nanofibrous aerogels obtained by directional freezing [1].

Air Filtration

Particulate matter (PM) pollution cause serious harm to human health, and effective removal of PMs has become an urgent need in various fields. So far, various filtration materials have been developed, and ceramic fiber-based filters are offer a advanced filtration technology developed in recent years, comparatively [4, 5, 7, 20, 98]. Because ceramic fibers have larger specific surface area and smaller pore diameter, they exhibit higher filtration efficiency and lower gas resistance to PMs compared to traditional granular filters and foam ceramic filter materials. Compared with polymer fiber filters, the ceramic fiber filters offer a better chemical stability, and high temperature resistance, demonstrating more advantages in the field of high temperature flue gas filtration.

In 2018, Wang et al. [5] developed an elastic, high-temperature resistant and high-efficiency air filter based on yttrium-stabilized zirconia (YSZ) nanofiber sponges using solution blow spinning technology. The YSZ nanofiber sponges exhibit a filtration efficiency of 99.4% and a pressure drop of only 57 Pa for NaCl particles in the range of 20–600 nm at a flow velocity of 4.8 cm s^{-1} at room temperature (Fig. 10a). They also tested the filtration properties of the YSZ nanofiber sponges at 750 °C. After filtration, the concentration of PMs with different particle sizes decreased significantly (Fig. 10b). When the airflow velocity was 10 cm s^{-1}, the filtration efficiency of the sponges to $PM_{0.3–2.5}$ and $PM_{2.5–10}$ was 99.97% and 99.98%, respectively (Fig. 10c). Therefore, ceramic nanofiber sponges have a potential application prospect in the field of high temperature PM filtration.

In the same year, Zhang et al. [98] developed hydroxyapatite nanowire-based aerogels with excellent elasticity, high porosity and low density. The aerogels demonstrated good biocompatibility and mechanical properties, high $PM_{2.5}$ filtration efficiency, and low pressure drop. They designed a series of breathing masks based on the hydroxyapatite

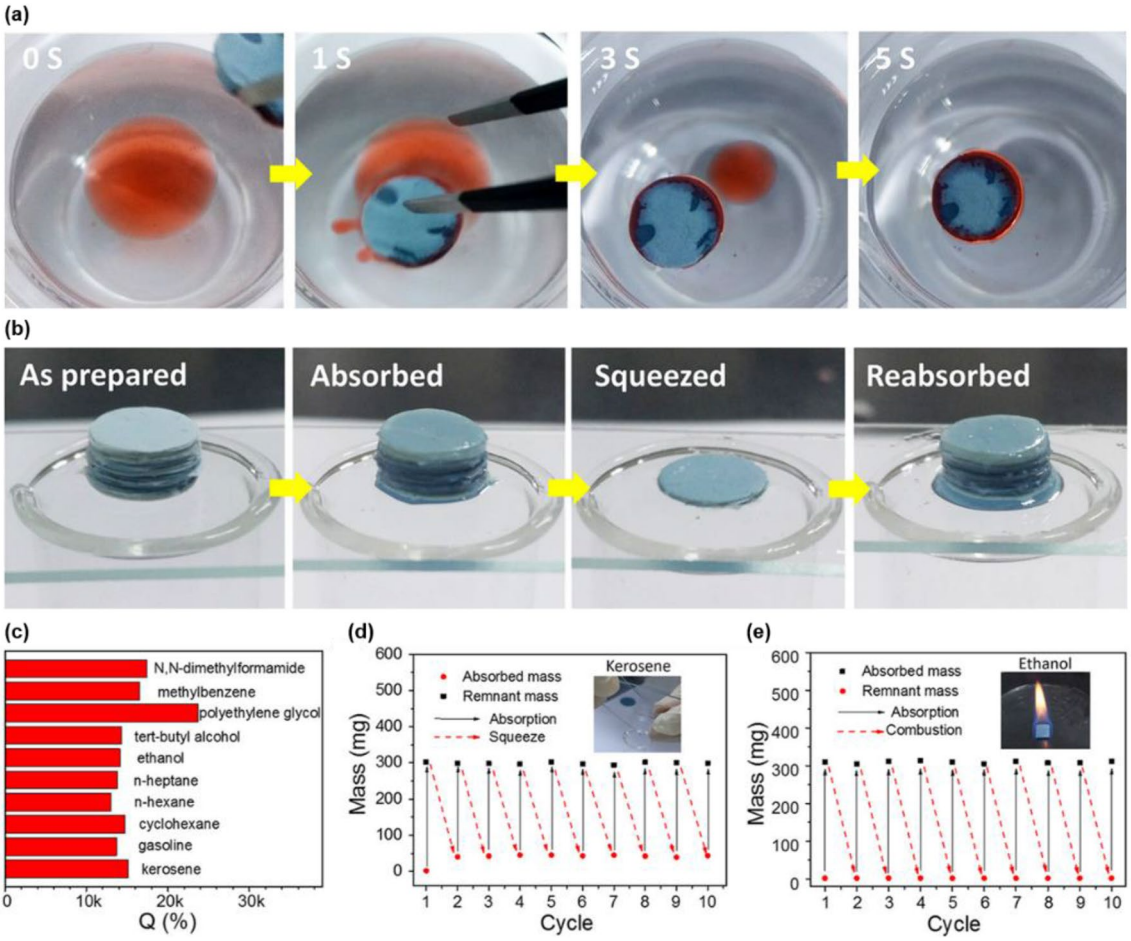

Fig. 11 Absorption properties of SiC nanowire aerogels to oil and organic solvents. **a** Digital image showing the absorption process of SiC nanowire aerogel to kerosene (kerosene was stained with Sudan III). **b** Digital image showing the repeatability of the absorption process. **c** Absorption capability of the SiC nanowire aerogels to various organic solvents. Recyclability of the SiC nanowire aerogels via **d** squeezing of the absorbed kerosene and **e** burning the absorbed ethanol. Reproduced with permission from Ref. [6]. Copyright 2018, American Chemical Society

nanowire aerogels (Fig. 10d), indicating that the aerogels promise great application in the field of personal protection.

An important progress about the preparation of FCFs was made in 2020, and an Al_2O_3-stabilized ZrO_2 (ASZ) fiber filter paper, with excellent flexibility and high temperature resistance of up to 1100 °C was developed via solution blow spinning (Fig. 4h) [4]. The filter papers with an areal density of 56 mg cm^{-2} possess a high filtration efficiency of 99.56% and a low pressure drop of 108 Pa to NaCl particles with a size of 15–615 nm at an airflow velocity of 5.4 cm s^{-1}, which combined with the high working temperature make the ceramic fiber papers promising in the field of high-temperature flue gas filtration (Fig. 10e).

Fiber materials have been widely used in the field of air filtration due to their excellent filtration properties. PMs can be removed from polluted gas by fiber materials through the mechanisms of direct interception, Brownian diffusion, inertial impacts, gravity settling, and electrostatic deposition. Additionally, fiber diameter has a significant effect on the filtration property [151], so in order to improve the filtration property of ceramic fiber materials, we need to overall prepare smaller diameter fibers. Besides, the cost effective ceramic fiber aerogels with excellent porosity can be used to develop high dust capacity filtering materials to increase their dust capacity.

Water Treatment

In order to solve the problems of oil spills and industrial organic solvent emissions, it is necessary to develop three-dimensional absorbent materials with excellent selectivity to absorb and remove organic pollutants from polluted water. Due to the excellent chemical and thermal stability, FCFs as

a new absorption material have been widely used to remove various organic pollutants in recent years [6–8, 89, 98].

Su et al. [6] prepared highly porous three-dimensional SiC nanowire aerogels via CVD method and used them as absorbents. Due to the low density and good hydrophobicity of the SiC nanowires aerogels, they can float on the surface of water after absorbing all the stained kerosene (Fig. 11a). Due to the excellent elasticity of the SiC nanowire aerogels, the absorbed organic solvents can be collected by squeezing the aerogel materials (Fig. 11b). The SiC nanowire aerogels exhibited a desired absorption selectivity and high absorption capacity (130–237 g g^{-1}), toward low viscosity organic solvents (Fig. 11c). The high absorption capacity of the SiC nanowire aerogels can be attributed to their high porosity and low density. In addition, the SiC nanowire aerogels can be reused either by squeezing or burning the absorbed organic solvents (Fig. 11d, e).

Ren et al. [7] prepared SiC/SiO_x core–shell nanofiber aerogels with three-dimensional porous structure by CVD method and layer-by-layer self-assembly. The aerogel materials can quickly absorb various organic solvents and oils with large absorption capacity and robust reusability. Song et al. [89] demonstrated that BN aerogels are highly hydrophobic and can absorb oil equivalent to 160 times their weight, and the aerogels can be reused by burning the absorbed oil in air. Xue et al. [8] developed a multifunctional cellular-network foam, which is made of interconnected nanotubular hexagonal BN architectures, using in situ CVD assisted by carbothermal reduction. The foams have a high capacity for absorption, separation and removal of various oils and organic chemicals in oil/water systems, and show a feasible recycling. In addition, hydroxyapatite nanowire aerogels are also an ideal oil–water separation material, and they can be used as an absorbing material to achieve continuous oil–water separation [98].

Based on the analysis of reported literature, ceramic fiber materials used for water treatment are mostly non-oxide ceramic fibers, including SiC fibers, BN fibers, etc. In addition, these ceramic fiber materials mainly absorb organic matters in polluted water in the form of aerogel to achieve the purpose of water treatment. Currently, common oxide ceramic fibers are rarely used in water treatment. Therefore, more efforts should be made to develop oxide ceramic fiber absorption materials or filtration materials to achieve low-cost wastewater treatment.

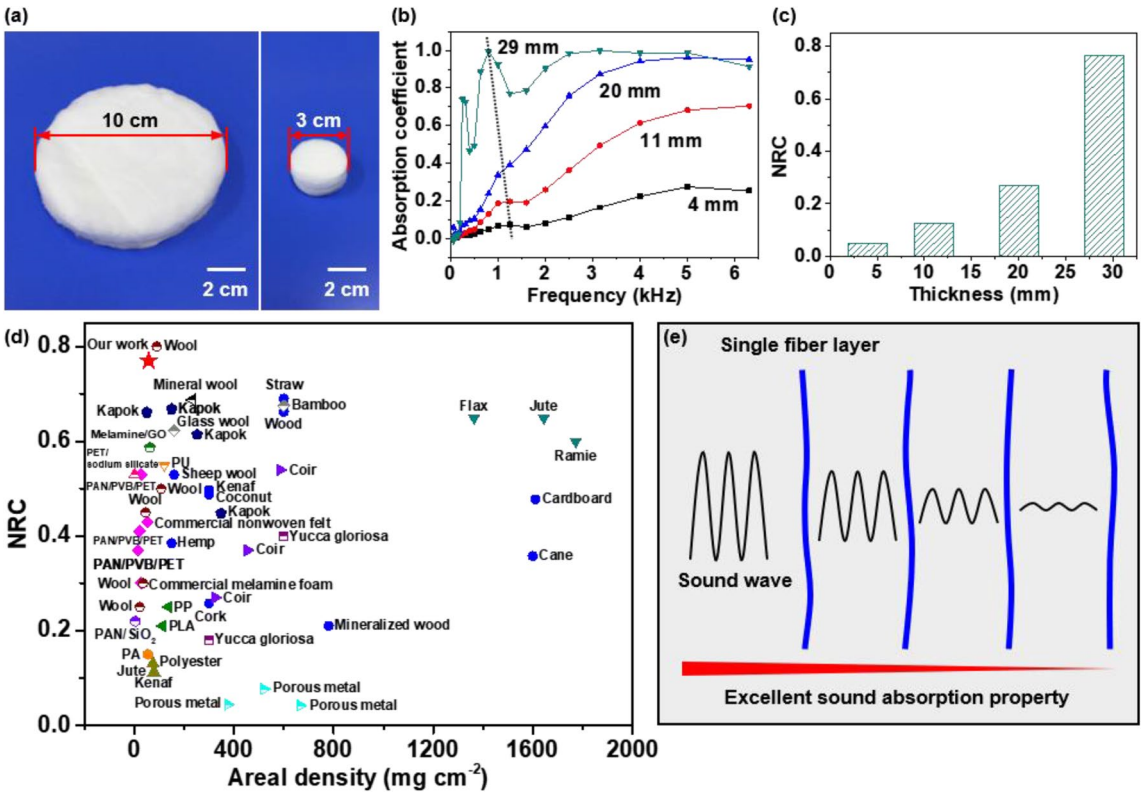

Fig. 12 Sound absorption application of SiO_2-Al_2O_3 composite fiber sponges. **a** Digital image of the sponges used to determine the sound absorption characteristic. **b** Sound absorption coefficient and **c** noise reduction coefficient (NRC) of the sponges with different thicknesses. **d** Comparison of sound absorption property of sponges with the other reported sound absorbing materials. **e** Schematic of the mechanism of the sound wave absorption in the sponges. Reproduced with permission from Ref. [3]. Copyright 2020, Springer Nature

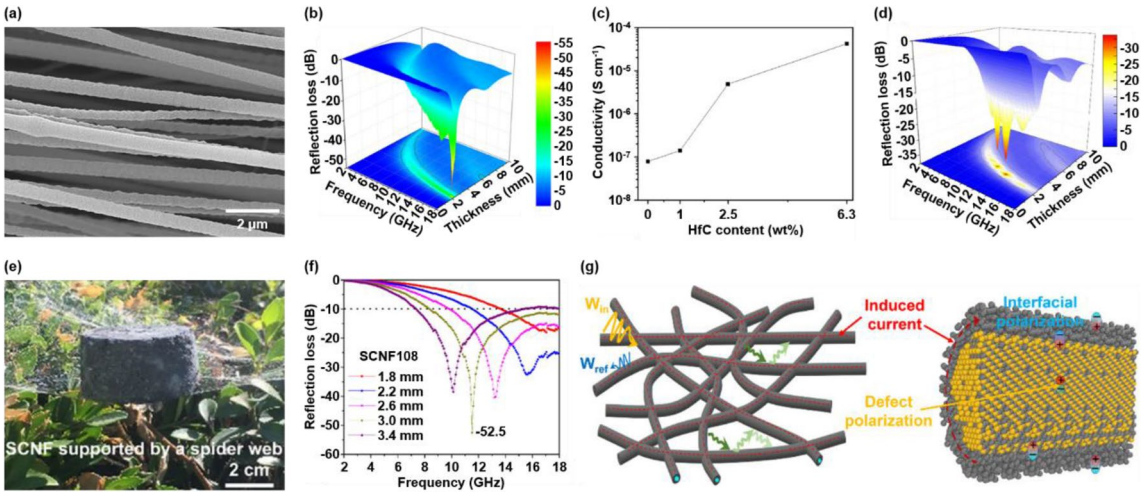

Fig. 13 Electromagnetic wave absorption application of FCFs. **a** SEM image of aligned SiC nanofibers. **b** Frequency and thickness dependance of RL for the composites with aligned SiC nanofibers. **c** Conductivity of the HfC/SiC nanofiber mats with different HfC contents. **d** Frequency and thickness dependance of RL for the silicon resin composites with HfC/SiC nanofibers (The content of HfC in the nanofibers is 2.5 wt%). **e** Digital image of a SCNF. **f** Frequency dependance of RL for the SCNFs with different thicknesses. **g** Schematic showing the electromagnetic wave absorption mechanism of the SCNFs. **a**, **b** Reproduced with permission from Ref. [136]. Copyright 2017, American Chemical Society. **c**, **d** Reproduced with permission from Ref. [137]. Copyright 2018, American Chemical Society. **e**–**g** Reproduced with permission from Ref. [132]. Copyright 2020, American Chemical Society

Sound Absorption

With the rapid development of urbanization and traffic, noise pollution from motor vehicles, mechanical equipment and engineering construction has become one of the most serious environmental problems. All kinds of noise greatly affect people's working efficiency and living standard. Sound absorption materials can be used to consume sound energy in the process of noise transmission, so the development of efficient sound absorption materials to eliminate or reduce noise pollution is of great significance. In addition, with the improvement of safety requirements, the flame retardancy requirements to sound absorption materials also improve continually, especially for the indoor and vehicle use, so it is urgent to develop efficient sound absorption materials with excellent flame retardant property.

Ceramic fiber materials have the characteristics of lightweight, non-combustibility, high temperature resistance and good chemical stability, so they are suitable for use as sound absorption material. We developed a superelastic SiO_2-Al_2O_3 composite fiber sponges with superior thermal insulation and sound absorption properties using solution blow spinning technology (Fig. 12a) [3]. The sound absorption coefficient and noise reduction coefficient (NRC) increased, by increasing the thickness of the sponges (Fig. 12b, c), as an sponge with an areal density of 58 mg cm^{-2} possesses an NRC value of 0.77, greater than most of the reported sound absorption materials (Fig. 12d). The superior sound absorption property of the sponges can be ascribed mainly to their low density and layered structure, and the sound waves can be absorbed multiple times in the sponges (Fig. 12e). In addition, the rough surface of the microfibers and the vibration of the microfibers caused by sound waves are also conducive to the sound energy absorption.

Electromagnetic Wave Absorption

With the rapid development of modern information technology, electromagnetic wave interference pollution has become more and more serious. It is of great importance to develop an absorbers with an acceptable level of electromagnetic wave absorption property. SiC fibers have become the most used electromagnetic wave absorption material because of their adjustable microstructure and dielectric property [72, 85, 131, 132, 134–137, 139, 152–155].

Hou et al. [136] developed SiC nanofiber mats with and without fiber alignment, via electrospinning and polymer precursor conversion (Fig. 13a). The 2.3 mm thick silicone resin composites with 5 wt% aligned SiC nanofibers exhibit a reflection loss (RL) of − 53 dB at the frequency of 17.6 GHz and the same composites with a thickness of 3 mm have an effective absorption bandwidth (EAB) of 8.6 GHz (Fig. 13b). The electromagnetic wave absorption properties of the composites with aligned SiC nanofibers outperforms the one with randomly decorated SiC nanofibers.

In addition to the orientation of the fibers, adding appropriate modifiers to the SiC fibers can also improve the electromagnetic wave absorption properties of the materials.

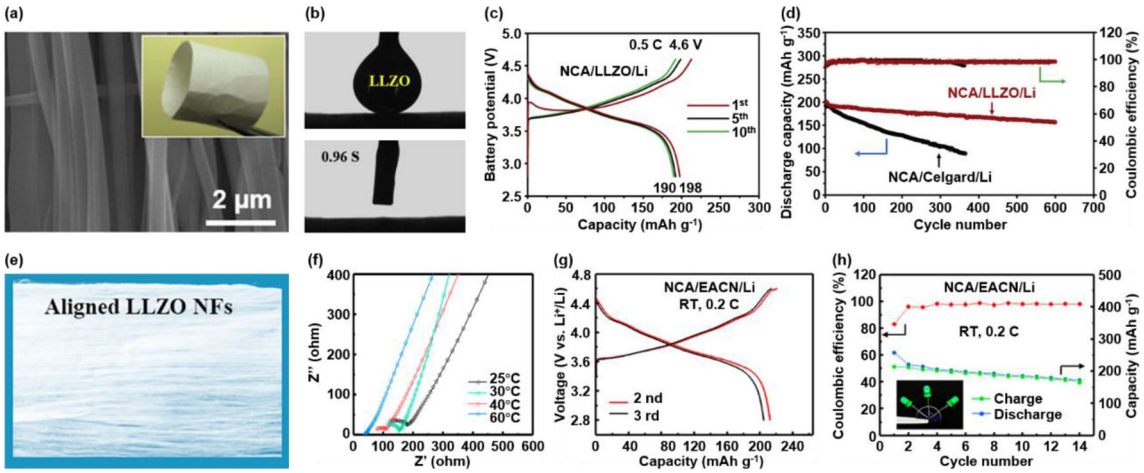

Fig. 14 Battery separator application of FCFs. **a** SEM image of the LLZO nanofiber films. (Inset is a photo of LLZO nanofiber film). **b** Digital images showing the electrolyte wettability of the LLZO nanofiber films. **c** Galvanostatic charge–discharge curves of the NCA/LLZO/Li battery with a termination charging voltage of 4.6 V at 0.5 C. **d** Cycling stability evaluation of discharge capacity and Coulombic efficiency for the NCA/LLZO/Li and NCA/Celgard/Li batteries. **e** Digital image of an Al-doped LLZO nanofiber film. **f** Electrochemical impedance spectroscopy of the composite electrolytes at different temperatures. **g** Charge–discharge curves of the solid-state NCA/EACN/Li batteries at 0.2 C. **h** Coulombic efficiency and capacity of the NCA/EACN/Li batteries at 0.2 C. **a**–**d** Reproduced with permission from Ref. [16]. Copyright 2019, Elsevier. **e**–**h** Reproduced with permission from Ref. [156]. Copyright 2019, Elsevier

Currently, iron (Fe) [139], Fe_3Si [135], Fe_3O_4 [154], hafnium carbide (HfC) [137], cobalt (Co) [134] have been reported as modifiers of SiC fibers. Taking HfC as an example, the addition of a small amount of HfC component in the SiC fibers can significantly improve the electrical conductivity of the fibers, thus improving the dielectric property and electromagnetic wave absorption property (Fig. 13c) [137]. The HfC/SiC nanofibers with 2.5wt% HfC in the 3 mm thick silicon resin composites show a minimal RL of -33.9 dB at 12.8 GHz and an EAB of 7.4 GHz (Fig. 13d).

Like the polymer precursor conversion, CVD is also a common procedure, for preparing the SiC fibers [6, 131, 132]. Cai et al. [132] developed three-dimensional porous SiC@C nanowire foams (SCNFs) by infiltrating glucose solution in CVD-constructed SiC nanowire aerogels and subsequent carbonization (Fig. 13e). The foams with a density of 108 mg cm^{-3} and a thickness of 3 mm exhibited a minimum RL value of -52.5 dB at the frequency of 11.5 GHz and a broad EAB of 10.1 GHz in the frequency range of 7.9–18 GHz (Fig. 13f). The excellent electromagnetic wave absorption properties of the foams can be attributed to their improved impedance match and multiscale energy dissipation mechanism (Fig. 13g).

Battery Separators

In recent years, with the development of battery technology, the safety of the battery is different systems has attracted more and more attention. Polymeric separators currently in use, are prone to causing serious safety incidents, mostly due to internal short circuits. Especially when thermal runaway occurs, the temperature inside the battery instantly reaches above 500 °C, where the polymer separators cannot withstand and degrades immediately. Therefore, it is important to develop ceramic fiber separators with high temperature resistance, especially for the advanced systems which work with battery.

Yan et al. [16] developed LLZO ceramic nanofiber films with silk-like softness, low density, and robust fire resistance via sol–gel electrospinning technique (Fig. 14a). The separators prepared from LLZO films, exhibit better electrolyte wettability than commercial Celgard 2500 separator and the electrolyte absorption rate is greater than 900% (Fig. 14b). The assembled Li-ion battery exhibited a wide electrochemical window of 2.7–4.6 V. When the termination charging voltage was increased to 4.6 V, the discharge capacity of the battery was increased to 190 mAh g^{-1} at 0.5 C (Fig. 14c). Compared with Celgard 2500-based battery, the LLZO-based battery demonstrated significantly stable capacity retention over 600 cycles (Fig. 14d).

A elastic and well-aligned $Li_{6.4}La_3Zr_2Al_{0.2}O_{12}$ (Al-doped LLZO) ceramic nanofiber web (EACN) was developed via sol–gel electrospinning and the composite electrolytes were prepared by combining the ceramic webs with ion-conducting polyvinylidene fluoride (PVDF) (Fig. 14e) [156]. Continuous ion transport channels are formed in the composite electrolytes, which enables them have high ionic conductivity of 1.16×10^{-4} S cm^{-1} at 30 °C (Fig. 14f). The solid-state battery NCA ($LiNi_{0.8}Co_{0.15}Al_{0.05}O_2$)/EACN/Li based on the Al-doped LLZO exhibited a high termination charging voltage of 4.6 V and large initial discharge capacity of 213 mAh

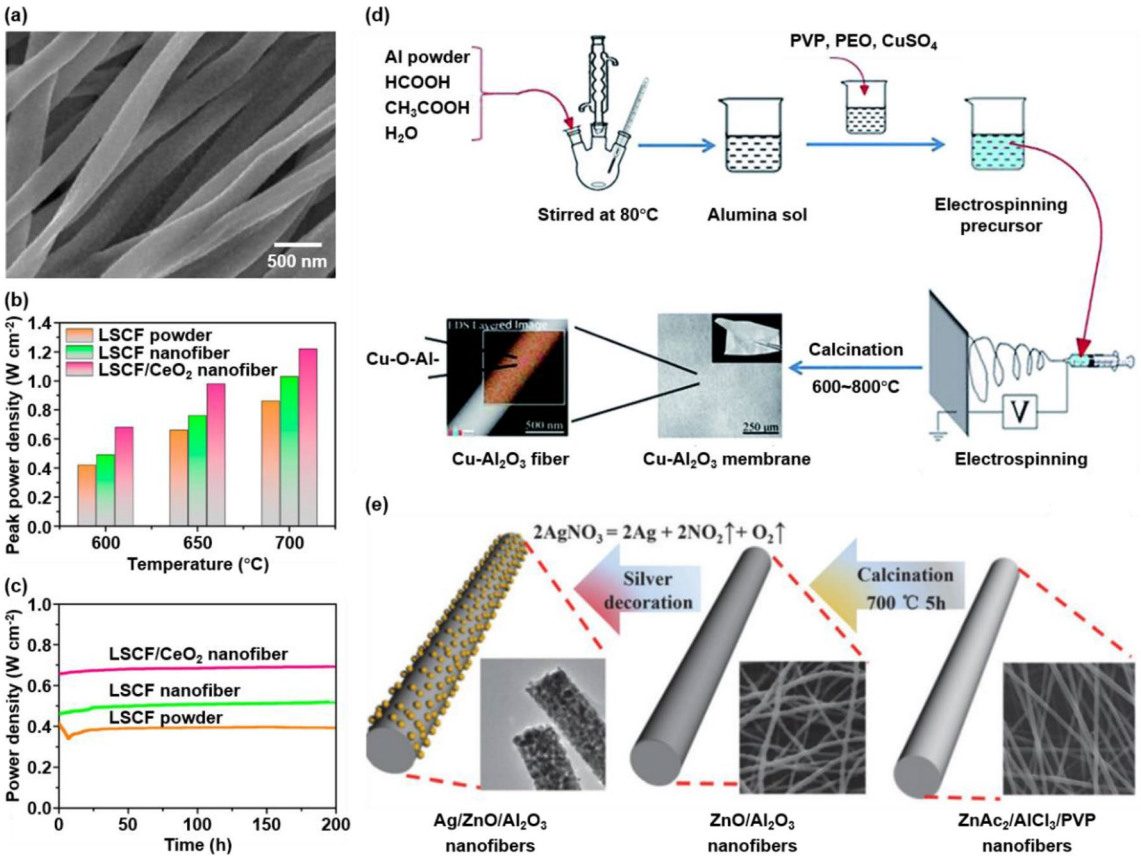

Fig. 15 Catalytic application of FCFs. **a** SEM image of LSCF/CeO_2 nanofibers. **b** Peak power density of the LSCF cathodes in the temperature range of 600–700 °C. **c** Stability evaluation of the single cells with LSCF cathodes under a constant voltage of 0.4 V at 600 °C. **d** Schematic showing the preparation of Cu-Al_2O_3 fibrous membranes. **e** Schematic showing the synthesis process of Ag/ZnO/γ-Al_2O_3 nanofibers. **a**–**c** Reproduced with permission from Ref. [157]. Copyright 2019, American Chemical Society. **d** Reproduced with permission from Ref. [161]. Copyright 2017, Royal Society of Chemistry. **e** Reproduced with permission from Ref. [162]. Copyright 2018, Royal Society of Chemistry

g^{-1} at 0.2 C (Fig. 14g). Multi-cycle test results show that the battery has a high Coulombic efficiency of > 95%, demonstrating a good electrochemical stability of the composite electrolytes (Fig. 14h).

Currently, there are few researches on the application of ceramic fibers in battery separator, most of which focus on LLZO fiber material. Given the excellent safety of ceramic fiber materials, more work should be devoted to developing more ceramic fiber-based separators with excellent electrochemical properties. In order to reduce the pore size of ceramic fiber-based battery separators and achieve better electrochemical property, it is an important research direction to develop ceramic fiber materials with smaller diameter.

Catalytic Application

Ceramic fiber materials have great application prospects in the field of catalysis because of their large specific surface area and good chemical and thermal stability [113]. The application of ceramic fibers in the field of catalysis has two forms. On the one hand, some ceramic materials possess good catalytic activity, and they can be applied in catalytic field by processing them into ceramic fibers [35, 38, 157–160]. On the other hand, ceramic fibers can be used as the carrier of catalysts, and ceramic fibers with catalytic activity can be obtained by loading catalysts on/in the ceramic fibers [161–164].

Ceramic materials that can be used to prepare ceramic fibers include TiO_2 [35, 38, 158, 160], CeO_2 [157], ZnO [158, 159], SnO_2 [159], perovskite-type oxide $La_{0.6}Sr_{0.4}Co_{0.2}Fe_{0.8}O_{3-\delta}$ (LSCF) [157], and so on. Zhang et al. [157] developed heterostructured LSCF/CeO_2 composite nanofibers via coaxial electrospinning, and these nanofibers can be used as cathode material of solid oxide fuel cells to improve their ORR activity and durability (Fig. 15a). Compared with the LSCF powders and nanofibers, the assembled cells with LSCF/CeO_2 composite nanofiber

cathodes exhibit much higher peak power density in the temperature range of 600–700 °C (Fig. 15b), and long-term stability under a voltage of 0.4 V at 600 °C (Fig. 15c).

There are two methods for preparing catalyst materials with ceramic fibers as the catalyst carrier. One method is to directly add catalysts or catalyst precursors to the spinning solution to obtain catalytic ceramic fibers by spinning and calcination [161, 163, 164]. For example, flexible self-standing Cu-Al_2O_3 fibrous membranes with high Fenton catalytic activity were prepared by electrospinning a spinning solution containing precursors of alumina and copper (Fig. 15d) [161]. Another alternative method is to obtain ceramic fibers by spinning and calcination first and then loading catalysts on the surface of the ceramic fibers [162]. Cheng et al. [162] first synthesized ZnO/γ-Al_2O_3 nanofibers via electrospinning and calcination. The Ag/ZnO/γ-Al_2O_3 nanofibers with efficient photocatalytic degradation property were further prepared by decorating silver nanoparticles on the surface of the ZnO/γ-Al_2O_3 nanofibers, by photoreduction and hydrothermal processes (Fig. 15e).

The preparation process of the first method for immobilizing catalysts is simple, but the catalysts are mainly distributed inside the fibers, which may affect the catalytic property of the catalysts, especially for these catalytic applications that require the catalysts to be exposed to the fiber surface, such as photocatalysis. In a general comparison, the second method for loading catalysts is slightly more complicated, but the catalysts are distributed on the surface of the fibers. This structure outstandingly improves the catalytic functionality of the catalysts can be fully.

Other Applications

Using piezoelectric effect to harvest energy from movement and to generate power using small wearable electronic devices is today a hot topic of society. Some ceramic materials can be processed into FCFs with excellent piezoelectric properties, such as $BaTiO_3$ [165], lead zirconate titanate ($PbZr_{0.52}Ti_{0.48}O_3$, PZT) [166], ZnO [167, 168], and (Na, K)NbO_3 [169–171]. These ceramic fibers exhibit excellent responses to the impacts, and that is why they found broad applications in piezoelectric nanogenerators, highly functional electromechanical sensors, transducers, and other wearable stress responding electrical devices.

Earth-rare elements and components are reported as the other ceramics, which can be used in fibers for various potential applications. The interesting functional properties of the earth-rare materials is arising from their unique 4f electron configuration and luminescence characteristics. A variety of earth-rare cations-doped luminescent ceramic fibers have been developed, including Eu^{3+}-doped Al_2O_3 nanofibers [172], Er^{3+}-doped $BaTiO_3$ nanofibers [173], $CaSi_2O_2N_2$:RE (RE = Ce^{3+}/Tb^{3+}, Eu^{2+}, Mn^{2+}) nanofibers [174], $La_2O_2CN_2$:Yb^{3+}/Tm^{3+} nanofibers [175], and $SrWO_4$:Sm^{3+} nanofibers [176]. In addition, some oxide ceramic fibers, such as GeO_2 fibers [177], TiO_2 nanofibers [178], and hollow $BaTiO_3$ nanofibers, demonstrate astonishing photoluminescence properties [179]. These luminescent materials can be utilized in the fields of sensors, transducers, white light-emitting diodes, and other luminescent devices.

Conclusions and Outlook

In the last decade or so, tremendous progresses have been witnessed in development and application of FCFs. Different types of materials have been processed into FCFs, such as oxide fibers, carbide fibers, nitride fibers and other ceramic fibers from the major categories. Many methods have been developed to prepare FCFs, including centrifugal spinning, electrospinning, solution blow spinning, self-assembly, chemical vapor deposition, atomic layer deposition, and polymer conversion. The rapid development of FCFs preparation has promoted the exploration of their applications in multiple different fields, including high temperature thermal insulation, air filtration, water treatment, sound absorption, electromagnetic wave absorption, battery separator, catalytic application, among others.

Some development directions and opportunities for FCFs should be noted.

1. For some preparation methods of FCFs, such as electrospinning and solution blow spinning, polymers need to be added to the spinning solution as thickeners and templates to assist in fiber forming. These polymer components should be eliminated by calcination, which usually leaves the ceramic fibers, as the final product. Also, elimination of polymers will result in a significant reduction of the fiber diameter, and a significant contraction of the three-dimensional bulk fiber materials can be observed macroscopically. This also dramatically wastes the resources, a dramatic, therefore, using the high molecular weight polymers as the template for the electrospinning is strongly suggested.
2. For some single-component ceramic materials, they are less flexible when processed into ceramic fibers. Flexibility of ceramic fibers can be improved by adding the other ceramic components. For example, adding some yttrium oxide, alumina, etc. to the zirconia fibers can effectively improve their flexibility [4, 5]. Therefore, development of multi-component ceramic fibers is an important approach to solve the rigidity of FCFs. The composite of different ceramic components not only can improve the flexibility of ceramic fibers, but also

enhances the other important properties, such as temperature resistance [3]. In addition, what we also need to do is to explore the use of low-cost ceramic precursors to prepare FCFs to reduce the cost of materials.

3. A certain shape is required for the practical application of FCFs, including one-dimensional yarns, two-dimensional films, and three-dimensional aerogels. Most of the preparation methods cannot obtain FCFs with regular shapes, and some methods can only obtain FCF films or webs. For those applications that require three-dimensional FCFs, such as thermal insulation and sound absorption, the FCF films need to be further processed, as they seriously limit their practical application. Among the discussed methods, solution blow spinning can readily obtain two-dimensional FCF films and three-dimensional FCF sponges, which should be more applied in future research.
4. In order to reduce the consumption of petroleum resources, polymers derived from natural materials can be used in the preparation of FCFs. On the one hand, in methods such as electrospinning and solution blow spinning that use spinning solutions, polymers derived from natural materials can be used as thickeners for spinning solutions and templates for FCFs. On the other hand, natural materials can be used as carbon or nitrogen sources for non-oxide FCFs in methods such as chemical vapor deposition.
5. For the electrospinning and solution blow spinning, the spinning devices with single or several nozzles can only be used for laboratory research, and it's difficult for them to meet the practical application requirements. In recent years, needleless electrospinning technology has been developed as an efficient technique for the large-scale preparation of ultrathin fibers [180]. However, currently the needleless electrospinning is mainly used in the preparation of polymer fibers. Therefore, it is urgent to expand the application of this technology in the large-scale production of ceramic fiber materials. In addition, it is of great significance to develop needle-free solution blow spinning technology and explore its application in the mass production of ceramic fibers.

Acknowledgements This study was supported by the National Natural Science Foundation of China (52102090, 52127805, 52073047), the Science and Technology Commission of Shanghai Municipality (20JC1414900), the Innovation Program of Shanghai Municipal Education Commission (2017-01-07-00-03-E00055), and the Program of Shanghai Academic/Technology Research Leader (20XD1433700).

Declarations

Conflict of interest The authors declare no competing financial interest.

References

1. Si Y, Wang X, Dou L, Yu J, Ding B. Ultralight and fire-resistant ceramic nanofibrous aerogels with temperature-invariant superelasticity. *Sci Adv* **2018**;*4*:eaas8925.
2. Wang H, Zhang X, Wang N, Li Y, Feng X, Huang Y, Zhao C, Liu Z, Fang M, Ou G, Gao H, Li X, Wu H. Ultralight, scalable, and high-temperature-resilient ceramic nanofiber sponges. *Sci Adv* **2017**;*3*:e1603170.
3. Jia C, Li L, Liu Y, Fang B, Ding H, Song J, Liu Y, Xiang K, Lin S, Li Z, Si W, Li B, Sheng X, Wang D, Wei X, Wu H. Highly compressible and anisotropic lamellar ceramic sponges with superior thermal insulation and acoustic absorption performances. *Nat Commun* **2020**;*11*:3732.
4. Jia C, Liu Y, Li L, Song J, Wang H, Liu Z, Li Z, Li B, Fang M, Wu H. A foldable all-ceramic air filter paper with high efficiency and high-temperature resistance. *Nano Lett* **2020**;*20*:4993–5000.
5. Wang H, Lin S, Yang S, Yang X, Song J, Wang D, Wang H, Liu Z, Li B, Fang M, Wang N, Wu H. High-temperature particulate matter filtration with resilient yttria-stabilized ZrO_2 nanofiber sponge. *Small* **2018**;*14*:e1800258.
6. Su L, Wang H, Niu M, Fan X, Ma M, Shi Z, Guo SW. Ultralight, recoverable, and high-temperature-resistant SiC nanowire aerogel. *ACS Nano* **2018**;*12*:3103–11.
7. Ren B, Liu J, Rong Y, Wang L, Lu Y, Xi X, Yang J. Nanofibrous aerogel bulk assembled by cross-linked SiC/SiO_x core-shell nanofibers with multifunctionality and temperature-invariant hyperelasticity. *ACS Nano* **2019**;*13*:11603–12.
8. Xue YM, Dai PC, Zhou M, Wang X, Pakdel A, Zhang C, Weng QH, Takei T, Fu XW, Popov ZI, Sorokin PB, Tang CC, Shimamura K, Bando Y, Golberg D. Multifunctional superelastic foam-like boron nitride nanotubular cellular-network architectures. *ACS Nano* **2017**;*11*:558–68.
9. Si Y, Yu J, Tang X, Ge J, Ding B. Ultralight nanofibre-assembled cellular aerogels with superelasticity and multifunctionality. *Nat Commun* **2014**;*5*:5802.
10. Wang F, Dou L, Dai J, Li Y, Huang L, Si Y, Yu J, Ding B. In situ synthesis of biomimetic silica nanofibrous aerogels with temperature-invariant superelasticity over one million compressions. *Angew Chem Int Ed Engl* **2020**;*59*:8285–92.
11. Mi HY, Jing X, Huang HX, Turng LS. Instantaneous self-assembly of three-dimensional silica fibers in electrospinning: Insights into fiber deposition behavior. *Mater Lett* **2017**;*204*:45–8.
12. Wang X, Dou L, Li Z, Yang L, Yu J, Ding B. Flexible hierarchical ZrO_2 nanoparticle-embedded SiO_2 nanofibrous membrane as a versatile tool for efficient removal of phosphate. *ACS Appl Mater Interfaces* **2016**;*8*:34668–76.
13. Mao X, Si Y, Chen Y, Yang L, Zhao F, Ding B, Yu J. Silica nanofibrous membranes with robust flexibility and thermal stability for high-efficiency fine particulate filtration. *RSC Adv* **2012**;*2*:12216–23.
14. Loccufier E, Geltmeyer J, Daelemans L, D'hooge DR, De Buysser K, De Clerck K. Silica nanofibrous membranes for the separation of heterogeneous azeotropes. *Adv Funct Mater* **2018**;*28*:1804138.
15. Huang T, Zhu Y, Zhu J, Yu H, Zhang Q, Zhu M. Self-reinforcement of light, temperature-resistant silica nanofibrous aerogels with tunable mechanical properties. *Adv Fiber Mater* **2020**;*2*:338–47.
16. Yan J, Zhao Y, Wang X, Xia S, Zhang Y, Han Y, Yu J, Ding B. Polymer template synthesis of soft, light, and robust oxide ceramic films. *Science* **2019**;*15*:185–95.

17. Lu B, He Y, Duan H, Zhang Y, Li X, Zhu C, Xie E. A new ultrahigh-speed method for the preparation of nanofibers containing living cells: a bridge towards industrial bioengineering applications. *Nanoscale* **2012**;*4*:1003–9.
18. Ren LY, Simmons TJ, Lu FY, Rahmi O, Kotha SP. Template free and large-scale fabrication of silica nanotubes with centrifugal jet spinning. *Chem Eng J* **2014**;*254*:39–45.
19. Ren L, Ozisik R, Kotha SP. Rapid and efficient fabrication of multilevel structured silica micro-/nanofibers by centrifugal jet spinning. *J Colloid Interface Sci* **2014**;*425*:136–42.
20. Tepekiran BN, Calisir MD, Polat Y, Akgul Y, Kilic A. Centrifugally spun silica (SiO_2) nanofibers for high-temperature air filtration. *Aerosol Sci Technol* **2019**;*53*:921–32.
21. Mahapatra A, Mishra BG, Hota G. Synthesis of ultrafine α-Al_2O_3 fibers via electrospinning method. *Ceram Int* **2011**;*37*:2329–33.
22. Wang Y, Li W, Xia Y, Jiao X, Chen D. Electrospun flexible self-standing gamma-alumina fibrous membranes and their potential as high-efficiency fine particulate filtration media. *J Mater Chem A* **2014**;*2*:15124–31.
23. Li L, Liu X, Wang G, Liu Y, Kang W, Deng N, Zhuang X, Zhou X. Research progress of ultrafine alumina fiber prepared by sol-gel method: a review. *Chem Eng J* **2021**;*421*:127744.
24. Wang Y, Li W, Jiao XL, Chen DR. Electrospinning preparation and adsorption properties of mesoporous alumina fibers. *J Mater Chem A* **2013**;*1*:10720–6.
25. Song XL, Zhang KC, Song Y, Duan ZX, Liu Q, Liu Y. Morphology, microstructure and mechanical properties of electrospun alumina nanofibers prepared using different polymer templates: A comparative study. *J Alloys Compd* **2020**;*829*:154502.
26. Li L, Kang W, Zhao Y, Li Y, Shi J, Cheng B. Preparation of flexible ultra-fine Al_2O_3 fiber mats via the solution blowing method. *Ceram Int* **2015**;*41*:409–15.
27. Sedaghat A, Taheri-Nassaj E, Naghizadeh R. An alumina mat with a nano microstructure prepared by centrifugal spinning method. *J Non-cryst Solids* **2006**;*352*:2818–28.
28. Akia M, Capitanachi D, Martinez M, Hernandez C, de Santiago H, Mao Y, Lozano K. Development and optimization of alumina fine fibers utilizing a centrifugal spinning process. *Microporous Mesoporous Mater* **2018**;*262*:175–81.
29. Sun G, Du X, Zhang M, Zhou C, Chen J, Liu F. Fabrication of zirconia fibers by a sol-gel combined rotational centrifugal spinning technique. *Trans Indian Ceram Soc* **2014**;*73*:228–32.
30. Ruiz-Rosas R, Bedia J, Rosas JM, Lallave M, Loscertales IG, Rodríguez-Mirasol J, Cordero T. Methanol decomposition on electrospun zirconia nanofibers. *Catal Today* **2012**;*187*:77–87.
31. Chen Y, Mao X, Shan H, Yang J, Wang H, Chen S, Tian F, Yu J, Ding B. Free-standing zirconia nanofibrous membranes with robust flexibility for corrosive liquid filtration. *RSC Adv* **2014**;*4*:2756–63.
32. Koo JY, Hwang S, Ahn M, Choi M, Byun D, Lee W. Controlling the diameter of electrospun yttria-stabilized zirconia nanofibers. *J Am Ceram Soc* **2016**;*99*:3146–50.
33. Liu H-Y, Chen Y, Liu G-S, Pei S-G, Liu J-Q, ji H, Wang R-D. Preparation of high-quality zirconia fibers by super-high rotational centrifugal spinning of inorganic sol. *Mater Manuf Processes*, **2013**;*28*:133–8.
34. Zhang M, Wang Y, Zhang Y, Song J, Si Y, Yan J, Ma C, Liu YT, Yu J, Ding B. Conductive and elastic TiO_2 nanofibrous aerogels: a new concept toward self-supported electrocatalysts with superior activity and durability. *Angew Chem, Int Ed* **2020**;*59*:2–11.
35. Zhang RZ, Wang XQ, Song J, Si Y, Zhuang XM, Yu JY, Ding B. In situ synthesis of flexible hierarchical TiO_2 nanofibrous membranes with enhanced photocatalytic activity. *J Mater Chem A* **2015**;*3*:22136–44.
36. Wu M-C, Sapi A, Avila A, Szabo M, Hiltunen J, Huuhtanen M, Toth G, Kukovecz A, Konya Z, Keiski R, Su W-F, Jantunen H, Kordas K. Enhanced photocatalytic activity of TiO_2 nanofibers and their flexible composite films: decomposition of organic dyes and efficient H_2 generation from ethanol-water mixtures. *Nano Res* **2011**;*4*:360–9.
37. Santos AMC, Mota MF, Leite RS, Neves GA, Medeiros ES, Menezes RR. Solution blow spun titania nanofibers from solutions of high inorganic/organic precursor ratio. *Ceram Int* **2018**;*44*:1681–9.
38. Gonzalez-Abrego M, Hernandez-Granados A, Guerrero-Bermea C, Martinez de la Cruz A, Garcia-Gutierrez D, Sepulveda-Guzman S, Cruz-Silva R. Mesoporous titania nanofibers by solution blow spinning. *J Sol-Gel Sci Technol*, **2017**;*81*:468–74.
39. Costa DL, Leite RS, Neves GA, de Lima Santana LN, Medeiros ES, Menezes RR. Synthesis of TiO_2 and ZnO nano and submicrometric fibers by solution blow spinning. *Mater Lett* **2016**;*183*:109–13.
40. Qian L, Willneff E, Zhang H. A novel route to polymeric submicron fibers and their use as templates for inorganic structures. *Chem Commun*, **2009**;3946–8.
41. Korhonen JT, Hiekkataipale P, Malm J, Karppinen M, Ikkala O, Ras RHA. Inorganic hollow nanotube aerogels by atomic layer deposition onto native nanocellulose templates. *ACS Nano* **2011**;*5*:1967–74.
42. Liu H, Chen Y, Pei S, Liu G, Liu J. Preparation of nanocrystalline titanium dioxide fibers using sol-gel method and centrifugal spinning. *J Sol-Gel Sci Technol* **2013**;*65*:443–51.
43. Bao N, Wei ZT, Ma ZH, Liu F, Yin GB. Si-doped mesoporous TiO_2 continuous fibers: preparation by centrifugal spinning and photocatalytic properties. *J Hazard Mater* **2010**;*174*:129–36.
44. Wang FY, Song LF, Zhang HC, Meng Y, Luo LQ, Xi Y, Liu L, Han N, Yang ZX, Tang J, Shan FK, Ho JC. ZnO nanofiber thin-film transistors with low-operating voltages. *Adv Electron Mater* **2018**;*4*:1700336.
45. Ning Y, Zhang ZM, Teng F, Fang XS. Novel transparent and self-powered UV photodetector based on crossed ZnO nanofiber array homojunction. *Small* **2018**;*14*:1703754.
46. Ahmad M, Pan CF, Luo ZX, Zhu J. A single ZnO nanofiber-based highly sensitive amperometric glucose biosensor. *J Phys Chem C* **2010**;*114*:9308–13.
47. Wang X, Zhao M, Liu F, Jia J, Li X, Cao L. C_2H_2 gas sensor based on Ni-doped ZnO electrospun nanofibers. *Ceram Int* **2013**;*39*:2883–7.
48. Liu RL, Dong X, Xie ST, Jia T, Xue YJ, Liu JC, Jing W, Guo AR. Ultralight, thermal insulating, and high-temperature-resistant mullite-based nanofibrous aerogels. *Chem Eng J* **2019**;*360*:464–72.
49. Zadeh MMA, Keyanpour-Rad M, Ebadzadeh T. Synthesis of mullite nanofibres by electrospinning of solutions containing different proportions of polyvinyl butyral. *Ceram Int* **2013**;*39*:9079–84.
50. Song XL, Ma YZ, Wang J, Liu B, Yao SW, Cai QS, Liu WS. Homogeneous and flexible mullite nanofibers fabricated by electrospinning through diphasic mullite sol-gel route. *J Mater Sci* **2018**;*53*:14871–83.
51. Xian L, Zhang Y, Wu Y, Zhang X, Dong X, Liu J, Guo A. Microstructural evolution of mullite nanofibrous aerogels with different ice crystal growth inhibitors. *Ceram Int* **2020**;*46*:1869–75.
52. Song XL, Liu WS, Wang J, Xu SH, Liu B, Cai QS, Ma YZ. Highly aligned continuous mullite nanofibers: conjugate electrospinning fabrication, microstructure and mechanical properties. *Mater Lett* **2018**;*212*:20–4.

53. da Costa Farias RM, Menezes RR, Oliveira JE, de Medeiros ES. Production of submicrometric fibers of mullite by solution blow spinning (SBS). *Mater Lett* **2015**;*149*:47–9.
54. Dai Y, Tian J, Fu W. Shape manipulation of porous CeO_2 nanofibers: facile fabrication, growth mechanism and catalytic elimination of soot particulates. *J Mater Sci* **2019**;*54*:10141–52.
55. Feng C, Lin X, Wang X, Liu H, Liu B, Zhu L, Zhang G, Xu D. Preparation, ferromagnetic and photocatalytic performance of NiO and hollow Co_3O_4 fibers through centrifugal-spinning technique. *Mater Res Bull* **2016**;*74*:319–24.
56. Wu H, Lin D, Pan W. Fabrication, assembly, and electrical characterization of CuO nanofibers. *Appl Phys Lett* **2006**;*89*:133125.
57. Wang H, Huang Y, Liao S, He H, Wu H. Tin oxide nanofiber and 3D sponge structure by blow spinning. *IOP Conf Ser Earth Environ Sci.* **2019**;*358*:052015.
58. Yan J, Han Y, Xia S, Wang X, Zhang Y, Yu J, Ding B. Polymer template synthesis of flexible $BaTiO_3$ crystal nanofibers. *Adv Funct Mater* **2019**;*29*:1907919.
59. Zhuang YY, Wei XY, Zhao Y, Li JL, Fu XT, Hu QY, Cui Y, Li F, Xu Z. Microstructure and elastic properties of $BaTiO_3$ nanofibers sintered in various atmospheres. *Ceram Int* **2018**;*44*:2426–31.
60. Ron LY, Kotha SP. Centrifugal jet spinning for highly efficient and large-scale fabrication of barium titanate nanofibers. *Mater Lett* **2014**;*117*:153–7.
61. Zhu P, Yan CY, Dirican M, Zhu JD, Zang J, Selvan RK, Chung CC, Jia H, Li Y, Kiyak Y, Wu NQ, Zhang XW. $Li_{0.33}La_{0.557}TiO_3$ ceramic nanofiber-enhanced polyethylene oxide-based composite polymer electrolytes for all-solid-state lithium batteries. *J Mater Chem A*. **2018**;*6*:4279–85.
62. Huang Z, Kolbasov A, Yuan Y, Cheng M, Xu Y, Rojaee R, Deivanayagam R, Foroozan T, Liu Y, Amine K, Lu J, Yarin AL, Shahbazian-Yassar R. Solution blowing synthesis of Li-conductive ceramic nanofibers. *ACS Appl Mater Interfaces* **2020**;*12*:16200–8.
63. Mohammadi M, Alizadeh P, Clemens FJ. Synthesis of $CaCu_3Ti_4O_{12}$ nanofibers by electrospinning. *Ceram Int* **2015**;*41*:13417–24.
64. Qin D, Liang G, Gu A. $CaCu_3Ti_4O_{12}$ electrospun fibre: a new form of $CaCu_3Ti_4O_{12}$ and its dielectric property. *J Alloys Compd* **2013**;*549*:11–7.
65. Mohammadi M, Alizadeh P, Clemens FJ. Effect of using different precursors on electrospinning of $CaCu_3Ti_4O_{12}$. *Ceram Int* **2016**;*42*:4690–9.
66. Liu J, Liu W, Ji SM, Zhou YC, Hodgson P, Li YC. Electrospun spinel $LiNi_{0.5}Mn_{1.5}O_4$ hierarchical nanofibers as 5V cathode materials for lithium-ion batteries. *ChemPlusChem* **2013**;*78*:636–41.
67. Xie Y, Wang L, Ma D, Peng Y, Zhu L, Wang X, Zhang G, Wang T, Jia Z, Zhang J. Preparation, mechanical properties, and diffuse reflectance of YAG continuous fibers and nanofibers. *Ceram Int* **2019**;*45*:21213–9.
68. Wang HL, Liao SY, Bai XP, Liu ZL, Fang MH, Liu T, Wang N, Wu H. Highly flexible indium tin oxide nanofiber transparent electrodes by blow spinning. *ACS Appl Mater Interfaces* **2016**;*8*:32661–6.
69. Zhang Q, Wu X, Chen HH, Yang B. Preparation and photoelectric properties of indium tin oxide depositional optical fiber by centrifugal spinning. *J Mater Sci: Mater Electron* **2015**;*26*:9031–6.
70. Rotta M, ZadoroSny L, Carvalho CL, Malmonge JA, Malmonge LF, Zadorosny R. YBCO ceramic nanofibers obtained by the new technique of solution blow spinning. *Ceram Int* **2016**;*42*:16230–4.
71. Silva VD, Ferreira LS, Simoes TA, Medeiros ES, Macedo DA. 1D hollow MFe_2O_4 (M=Cu, Co, Ni) fibers by solution blow spinning for oxygen evolution reaction. *J Colloid Interface Sci* **2019**;*540*:59–65.
72. An ZM, Ye CS, Zhang RB, Zhou P. Flexible and recoverable SiC nanofiber aerogels for electromagnetic wave absorption. *Ceram Int* **2019**;*45*:22793–801.
73. Liu Y, Liu Y, Choi WC, Chae S, Lee J, Kim B-S, Park M, Kim HY. Highly flexible, erosion resistant and nitrogen doped hollow SiC fibrous mats for high temperature thermal insulators. *J Mater Chem A* **2017**;*5*:2664–72.
74. Sarkar S, Zhai L. Polymer-derived non-oxide ceramic fibers-past, present and future. *Mater Express* **2011**;*1*:18–29.
75. Lu SL, Wang H, Niu M, Xu L, Ma M, Gao H, Cai Z, Fan X. Scalable fabrication of resilient SiC nanowires aerogels with exceptional high-temperature stability. *ACS Appl Mater Interfaces* **2019**;*11*:45338–44.
76. Li Y, Yan G, Zhao Y, Kang W, Li L, Zhuang X, Cheng B, Li X. Emulsion-blow spun self-sustained crystalline β-silicon carbide (SiC) fiber mat and its conductivity property. *Trans Indian Ceram Soc* **2017**;*76*:159–64.
77. Li F, Kang Z, Huang X, Zhang G-J. Fabrication of zirconium carbide nanofibers by electrospinning. *Ceram Int* **2014**;*40*:10137–41.
78. Cui XM, Nam YS, Lee JY, Park WH. Fabrication of zirconium carbide (ZrC) ultra-thin fibers by electrospinning. *Mater Lett* **2008**;*62*:1961–4.
79. Wang Y, Han C, Zheng D, Lei Y. Large-scale, flexible and high-temperature resistant ZrO_2/SiC ultrafine fibers with a radial gradient composition. *J Mater Chem A* **2014**;*2*:9607–12.
80. Cao S, Xie Z, Wang J, Wang H. Synthesis and characterization of polyzirconocarbosilane precursor. *Acta Polym Sin*, **2008**;621–5.
81. Wu N, Wan LY, Wang YD, Ko F. Conversion of hydrophilic SiOC nanofibrous membrane to robust hydrophobic materials by introducing palladium. *Appl Surf Sci* **2017**;*425*:750–7.
82. Guo AR, Roso M, Modesti M, Maire E, Adrien J, Colombo P. Characterization of porosity, structure, and mechanical properties of electrospun SiOC fiber mats. *J Mater Sci* **2015**;*50*:4221–31.
83. Guo AR, Roso M, Modesti M, Liu JC, Colombo P. Preceramic polymer-derived SiOC fibers by electrospinning. *J Appl Polym Sci* **2014**;*131*:39836.
84. Dong X, Liu RL, Dong W, Wang ZP, Guo AR, Liu JC, Chen C, Jiang Y. Fabrication and properties of lightweight SiOC fiber-based assembly aerogels with hierarchical pore structure. *Ceram Int* **2018**;*44*:22760–6.
85. Wang P, Cheng L, Zhang L. Lightweight, flexible SiCN ceramic nanowires applied as effective microwave absorbers in high frequency. *Chem Eng J* **2018**;*338*:248–60.
86. Flores O, Bordia RK, Nestler D, Krenkel W, Motz G. Ceramic fibers based on SiC and SiCN systems: current research, development, and commercial status. *Adv Eng Mater* **2014**;*16*:621–36.
87. Zheng C, Li X, Yu Y, Wang H, Cao F, Zhao D. Study of high temperature resistant SiC(Al) fibers precursor—polyaluminocarbosilane fibers. *Acta Polym Sin*, **2006**;768–73.
88. Li G, Zhu M, Gong W, Du R, Eychmüller A, Li T, Lv W, Zhang X. Boron nitride aerogels with super-flexibility ranging from liquid nitrogen temperature to 1000°C. *Adv Funct Mater* **2019**;*29*:1900188.
89. Song Y, Li B, Yang S, Ding G, Zhang C, Xie X. Ultralight boron nitride aerogels via template-assisted chemical vapor deposition. *Sci Rep* **2015**;*5*:10337.
90. Wang M, Zhang T, Mao D, Yao Y, Zeng X, Ren L, Cai Q, Mateti S, Li LH, Zeng X, Du G, Sun R, Chen Y, Xu JB, Wong CP. Highly compressive boron nitride nanotube aerogels reinforced with reduced graphene oxide. *ACS Nano* **2019**;*13*:7402–9.
91. Su L, Li M, Wang H, Niu M, Lu, Cai Z. Resilient Si_3N_4 nanobelt aerogel as fire-resistant and electromagnetic

wave-transparent thermal insulator. *ACS Appl Mater Interfaces* **2019**;*11*:15795–803.
92. Huo WL, Zhang XY, Xu J, Hu ZL, Yan S, Gan K, Yang JL. In situ synthesis of three-dimensional nanofiber-knitted ceramic foams via reactive sintering silicon foams. *J Am Ceram Soc* **2019**;*102*:2245–50.
93. Zhang XY, Huo WL, Chen Y, Hu ZL, Wang YL, Gan K, Yang JL. Novel micro-spherical Si_3N_4 nanowire sponges from carbon-doped silica sol foams via reverse templating method. *J Am Ceram Soc* **2019**;*102*:962–9.
94. Wu H, Sun Y, Lin DD, Zhong R, Zhang C, Pan W. GaN nanofibers based on electrospinning: facile synthesis, controlled assembly, precise doping, and application as high performance UV photodetector. *Adv Mater* **2009**;*21*:227–31.
95. Lin D, Wu H, Zhang R, Pan W. Preparation of ZnS nanofibers via electrospinning. *J Am Ceram Soc* **2007**;*90*:3664–6.
96. Hayase G, Nonomura K, Hasegawa G, Kanamori K, Nakanishi K. Ultralow-density, transparent, superamphiphobic boehmite nanofiber aerogels and their alumina derivatives. *Chem Mater* **2015**;*27*:3–5.
97. Chen FF, Zhu YJ, Chen F, Dong LY, Yang RL, Xiong ZC. Fire alarm wallpaper based on fire-resistant hydroxyapatite nanowire inorganic paper and graphene oxide thermosensitive sensor. *ACS Nano* **2018**;*12*:3159–71.
98. Zhang YG, Zhu YJ, Xiong ZC, Wu J, Chen F. Bioinspired ultralight inorganic aerogel for highly efficient air filtration and oil-water separation. *ACS Appl Mater Interfaces* **2018**;*10*:13019–27.
99. Mali SS, Patil PS, Hong CK. Low-cost electrospun highly crystalline kesterite Cu_2ZnSnS_4 nanofiber counter electrodes for efficient dye-sensitized solar cells. *ACS Appl Mater Interfaces* **2014**;*6*:1688–96.
100. Schuetz P, Alves AK, Bergmann CP. Effect of the in-air heat treatment in the phase formation and morphology of electrospun Cu_2ZnSnS_4 fibers. *Ceram Int* **2014**;*40*:11551–7.
101. Altecor A, Li Q, Lozano K, Mao Y. Mixed-valent VO_x/polymer nanohybrid fibers for flexible energy storage materials. *Ceram Int* **2014**;*40*:5073–7.
102. Zhang X, Lu Y. Centrifugal spinning: an alternative approach to fabricate nanofibers at high speed and low cost. *Polym Rev* **2014**;*54*:677–701.
103. Calisir MD, Kilic A. A comparative study on SiO_2 nanofiber production via two novel non-electrospinning methods: centrifugal spinning vs solution blowing. *Mater Lett* **2020**;*258*:126751.
104. Liu H, Zhou X, Chen Y, Li T, Pei S. Titanium dioxide fibers prepared by sol-gel process and centrifugal spinning. *J Sol-Gel Sci Technol* **2014**;*71*:102–8.
105. Altecor A, Mao YB, Lozano K. Large-scale synthesis of tin-doped indium oxide nanofibers using water as solvent. *Funct Mater Lett* **2012**;*5*:1250020.
106. Salinas A, Lizcano M, Lozano K. Synthesis of β-SiC fine fibers by the forcespinning method with microwave irradiation. *J Ceram* **2015**;*2015*:1–5.
107. Mahalingam S, Pierin G, Colombo P, Edirisinghe M. Facile one-pot formation of ceramic fibres from preceramic polymers by pressurised gyration. *Ceram Int* **2015**;*41*:6067–73.
108. Akia M, Mkhoyan KA, Lozano K. Synthesis of multiwall α-Fe_2O_3 hollow fibers via a centrifugal spinning technique. *Mater Sci Eng, C* **2019**;*102*:552–7.
109. Akia M, Salinas N, Luna S, Medina E, Valdez A, Lopez J, Ayala J, Alcoutlabi M, Lozano K. In situ synthesis of Fe_3O_4-reinforced carbon fiber composites as anodes in lithium-ion batteries. *J Mater Sci* **2019**;*54*:13479–90.
110. Wu H, Pan W, Lin DD, Li HP. Electrospinning of ceramic nanofibers: fabrication, assembly and applications. *J Adv Ceram* **2012**;*1*:2–23.
111. Luo CJ, Stoyanov SD, Stride E, Pelan E, Edirisinghe M. Electrospinning versus fibre production methods: from specifics to technological convergence. *Chem Soc Rev* **2012**;*41*:4708–35.
112. Homaeigohar S, Davoudpour Y, Habibi Y, Elbahri M. The electrospun ceramic hollow nanofibers. *Nanomaterials* **2017**;*7*:383.
113. Dai Y, Liu W, Formo E, Sun Y, Xia Y. Ceramic nanofibers fabricated by electrospinning and their applications in catalysis, environmental science, and energy technology. *Polym Adv Technol* **2011**;*22*:326–38.
114. Malwal D, Gopinath P. Fabrication and applications of ceramic nanofibers in water remediation: a review. *Crit Rev Environ Sci Technol* **2016**;*46*:500–34.
115. Xue JJ, Xie JW, Liu WY, Xia YN. Electrospun nanofibers: new concepts, materials, and applications. *Acc Chem Res* **2017**;*50*:1976–87.
116. Esfahani H, Jose R, Ramakrishna S. Electrospun ceramic nanofiber mats today: synthesis, properties, and applications. *Materials* **2017**;*10*:1238.
117. Li D, McCann JT, Xia YN. Electrospinning: a simple and versatile technique for producing ceramic nanofibers and nanotubes. *J Am Ceram Soc* **2006**;*89*:1861–9.
118. Shin YM, Hohman MM, Brenner MP, Rutledge GC. Experimental characterization of electrospinning: the electrically forced jet and instabilities. *Polymer* **2001**;*42*:9955–67.
119. Choi SS, Lee SG, Im SS, Kim SH, Joo YL. Silica nanofibers from electrospinning/sol-gel process. *J Mater Sci Lett* **2003**;*22*:891–3.
120. Lee SW, Kim YU, Choi SS, Park TY, Joo YL, Lee SG. Preparation of SiO_2/TiO_2 composite fibers by sol-gel reaction and electrospinning. *Mater Lett* **2007**;*61*:889–93.
121. Ye B, Jia C, Li Z, Li L, Zhao Q, Wang J, Wu H. Solution-blow spun PLA/SiO_2 nanofiber membranes toward high efficiency oil/water separation. *J Appl Polym Sci* **2020**;*137*:e49103.
122. Wang HY, Lin S, Zu D, Song JN, Liu ZL, Li L, Jia C, Bai XP, Liu JC, Li ZW, Wang D, Huang Y, Fang MH, Lei M, Li B, Wu H. Direct blow spinning of flexible and transparent Ag nanofiber heater. *Adv Mater Technol* **2019**;*4*:1900045.
123. Jia C, Li L, Song J, Li Z, Wu H. Mass production of ultrafine fibers by a versatile solution blow spinning method. *Acc Mater Res* **2021**;*2*:432–46.
124. Daristotle JL, Behrens AM, Sandler AD, Kofinas P. A review of the fundamental principles and applications of solution blow spinning. *ACS Appl Mater Interfaces* **2016**;*8*:34951–63.
125. Huang Y, Song JN, Yang C, Long YZ, Wu H. Scalable manufacturing and applications of nanofibers. *Mater Today* **2019**;*28*:98–113.
126. Medeiros ES, Glenn GM, Klamczynski AP, Orts WJ, Mattoso LHC. Solution blow spinning: a new method to produce micro- and nanofibers from polymer solutions. *J Appl Polym Sci* **2009**;*113*:2322–30.
127. Lou H, Han W, Wang X. Numerical study on the solution blowing annular jet and its correlation with fiber morphology. *Ind Eng Chem Res* **2014**;*53*:2830–8.
128. Li L, Xu CS, Chang RZ, Yang C, Jia C, Wang L, Song JN, Li ZW, Zhang FS, Fang B, Wei XD, Wang HB, Wu Q, Chen ZF, He XM, Feng XN, Wu H, Ouyang MG. Thermal-responsive, super-strong,

ultrathin firewalls for quenching thermal runaway in high-energy battery modules. *Energy Storage Mater* **2021**;*40*:329–36.
129. Meza LR, Das S, Greer JR. Strong, lightweight, and recoverable three-dimensional ceramic nanolattices. *Science* **2014**;*345*:1322–6.
130. Xu CC, Wang HL, Song JA, Bai XP, Liu ZL, Fang MH, Yuan YS, Sheng JY, Li XY, Wang N, Wu H. Ultralight and resilient Al_2O_3 nanotube aerogels with low thermal conductivity. *J Am Ceram Soc* **2018**;*101*:1677–83.
131. Cai Z, Su L, Wang H, Niu M, Tao L, Lu, Xu L, Li M, Gao H. Alternating multilayered Si_3N_4/SiC aerogels for broadband and high-temperature electromagnetic wave absorption up to 1000°C. *ACS Appl Mater Interfaces* **2021**;*13*:16704–12.
132. Cai Z, Su L, Wang H, Niu M, Gao H, Lu D, Li M. Hydrophobic SiC@C nanowire foam with broad-band and mechanically controlled electromagnetic wave absorption. *ACS Appl Mater Interfaces* **2020**;*12*:8555–62.
133. Ichikawa H. Polymer-derived ceramic fibers. *Annu Rev Mater Res* **2016**;*46*:335–56.
134. Hou Y, Yang Y, Deng CR, Li CJ, Wang CF. Implications from broadband microwave absorption of metal-modified SiC fiber mats. *ACS Appl Mater Interfaces* **2020**;*12*:31823–9.
135. Hou Y, Zhang Y, Du X, Yang Y, Deng C, Yang Z, Zheng L, Cheng L. Flexible Fe_3Si/SiC ultrathin hybrid fiber mats with designable microwave absorption performance. *RSC Adv* **2018**;*8*:33574–82.
136. Hou Y, Cheng LF, Zhang YN, Yang Y, Deng CR, Yang ZH, Chen Q, Du XQ, Zheng LX. SiC nanofiber mat: a broad-band microwave absorber, and the alignment effect. *ACS Appl Mater Interfaces* **2017**;*9*:43072–80.
137. Hou Y, Cheng L, Zhang Y, Yang Y, Deng C, Yang Z, Chen Q, Du X, Zhao C, Zheng L. Enhanced flexibility and microwave absorption properties of HfC/SiC nanofiber mats. *ACS Appl Mater Interfaces* **2018**;*10*:29876–83.
138. Miele P, Bernard S, Cornu D, Toury B. Recent developments in polymer-derived ceramic fibers (PDCFs): preparation, properties and applications - a review. *Soft Mater* **2007**;*4*:249–86.
139. Hou Y, Cheng L, Zhang Y, Yang Y, Deng C, Yang Z, Chen Q, Wang P, Zheng L. Electrospinning of Fe/SiC hybrid fibers for highly efficient microwave absorption. *ACS Appl Mater Interfaces* **2017**;*9*:7265–71.
140. Ge M, Lv XX, Zhang H, Yu SQ, Lu ZX, Zhang WG. Microstructures of a SiC-ZrC ceramic fiber derived from a polymeric precursor. *Materials* **2020**;*13*:2142.
141. Brown TD, Dalton PD, Hutmacher DW. Direct writing by way of melt electrospinning. *Adv Mater* **2011**;*23*:5651–7.
142. Robinson TM, Hutmacher DW, Dalton PD. The next frontier in melt electrospinning: taming the jet. *Adv Funct Mater* **2019**;*29*:1904664.
143. Li D, Xia YN. Direct fabrication of composite and ceramic hollow nanofibers by electrospinning. *Nano Lett* **2004**;*4*:933–8.
144. Qiu Y, Yu J, Rafique J, Yin J, Bai X, Wang E. Large-scale production of aligned long boron nitride nanofibers by multijet/multicollector electrospinning. *J Phys Chem C* **2009**;*113*:11228–34.
145. Geltmeyer J, Van der Schueren L, Goethals F, De Buysser K, De Clerck K. Optimum sol viscosity for stable electrospinning of silica nanofibres. *J Sol-Gel Sci Technol* **2013**;*67*:188–95.
146. Chapman BS, Mishra SR, Tracy JB. Direct electrospinning of titania nanofibers with ethanol. *Dalton Trans* **2019**;*48*:12822–7.
147. Geltmeyer J, De Roo J, Van den Broeck F, Martins JC, De Buysser K, De Clerck K. The influence of tetraethoxysilane sol preparation on the electrospinning of silica nanofibers. *J Sol-Gel Sci Technol* **2016**;*77*:453–62.
148. Dou L, Zhang X, Cheng X, Ma Z, Wang X, Si Y, Yu J, Ding B. Hierarchical cellular structured ceramic nanofibrous aerogels with temperature-invariant superelasticity for thermal insulation. *ACS Appl Mater Interfaces* **2019**;*11*:29056–64.
149. Xu X, Fu S, Guo J, Li H, Huang Y, Duan X. Elastic ceramic aerogels for thermal superinsulation under extreme conditions. *Mater Today* **2021**;*42*:162–77.
150. Su L, Wang H, Niu M, Dai S, Cai Z, Yang B, Huyan H, Pan X. Anisotropic and hierarchical SiC@SiO_2 nanowire aerogel with exceptional stiffness and stability for thermal superinsulation. *Sci Adv* **2020**;*6*:eaay6689.
151. Li P, Wang C, Zhang Y, Wei F. Air filtration in the free molecular flow regime: a review of high-efficiency particulate air filters based on carbon nanotubes. *Small* **2014**;*10*:4543–61.
152. Wang P, Cheng L, Zhang Y, Wu H, Hou Y, Yuan W, Zheng L. Flexible, hydrophobic SiC ceramic nanofibers used as high frequency electromagnetic wave absorbers. *Ceram Int* **2017**;*43*:7424–35.
153. Han MK, Yin XW, Hou ZX, Song CQ, Li XL, Zhang LT, Cheng LF. Flexible and thermostable graphene/SiC nanowire foam composites with tunable electromagnetic wave absorption properties. *ACS Appl Mater Interfaces* **2017**;*9*:11803–10.
154. Liang C, Liu C, Wang H, Wu L, Jiang Z, Xu Y, Shen B, Wang Z. SiC-Fe_3O_4 dielectric-magnetic hybrid nanowires: controllable fabrication, characterization and electromagnetic wave absorption. *J Mater Chem A* **2014**;*2*:16397–402.
155. Wang H, Wu L, Jiao J, Zhou J, Xu Y, Zhang H, Jiang Z, Shen B, Wang Z. Covalent interaction enhanced electromagnetic wave absorption in SiC/Co hybrid nanowires. *J Mater Chem A* **2015**;*3*:6517–25.
156. Zhao Y, Yan J, Cai W, Lai Y, Song J, Yu J, Ding B. Elastic and well-aligned ceramic LLZO nanofiber based electrolytes for solid-state lithium batteries. *Energy Storage Mater* **2019**;*23*:306–13.
157. Zhang W, Wang H, Guan K, Wei Z, Zhang X, Meng J, Liu X, Meng J. $La_{0.6}Sr_{0.4}Co_{0.2}Fe_{0.8}O_{3-\delta}/CeO_2$ heterostructured composite nanofibers as a highly active and robust cathode catalyst for solid oxide fuel cells. *ACS Appl Mater Interfaces* **2019**;*11*:26830–41.
158. Liu R, Ye H, Xiong X, Liu H. Fabrication of TiO_2/ZnO composite nanofibers by electrospinning and their photocatalytic property. *Mater Chem Phys* **2010**;*121*:432–9.
159. Liu R, Huang Y, Xiao A, Liu H. Preparation and photocatalytic property of mesoporous ZnO/SnO_2 composite nanofibers. *J Alloys Compd* **2010**;*503*:103–10.
160. Chuangchote S, Jitputti J, Sagawa T, Yoshikawa S. Photocatalytic activity for hydrogen evolution of electrospun TiO_2 nanofibers. *ACS Appl Mater Interfaces* **2009**;*1*:1140–3.
161. Wang Y, Li J, Sun JY, Wang YB, Zhao X. Electrospun flexible self-standing Cu-Al_2O_3 fibrous membranes as fenton catalysts for bisphenol A degradation. *J Mater Chem A* **2017**;*5*:19151–8.
162. Cheng Z, Zhao S, Han L. A novel preparation method for ZnO/γ-Al_2O_3 nanofibers with enhanced absorbability and improved photocatalytic water-treatment performance by Ag nanoparticles. *Nanoscale* **2018**;*10*:6892–9.

163. Jeong YJ, Koo WT, Jang JS, Kim DH, Cho HJ, Kim ID. Chitosan-templated Pt nanocatalyst loaded mesoporous SnO_2 nanofibers: a superior chemiresistor toward acetone molecules. *Nanoscale* **2018**;*10*:13713–21.
164. Patel AC, Li S, Wang C, Zhang W, Wei Y. Electrospinning of porous silica nanofibers containing silver nanoparticles for catalytic applications. *Chem Mater* **2007**;*19*:1231–8.
165. Yan J, Jeong YG. High performance flexible piezoelectric nanogenerators based on $BaTiO_3$ nanofibers in different alignment modes. *ACS Appl Mater Interfaces* **2016**;*8*:15700–9.
166. Lee H, Kim H, Kim DY, Seo Y. Pure piezoelectricity generation by a flexible nanogenerator based on lead zirconate titanate nanofibers. *ACS Omega* **2019**;*4*:2610–7.
167. Chen YQ, Zheng XJ, Feng X. The fabrication of vanadium-doped ZnO piezoelectric nanofiber by electrospinning. *Nanotechnology* **2010**;*21*:055708.
168. Cheng RR, Zhang CL, Chen WQ, Yang JS. Electrical behaviors of a piezoelectric semiconductor fiber under a local temperature change. *Nano Energy* **2019**;*66*:104081.
169. Kang HB, Chang J, Koh K, Lin LW, Cho YS. High quality Mn-doped (Na, K)NbO_3 nanofibers for flexible piezoelectric nanogenerators. *ACS Appl Mater Interfaces* **2014**;*6*:10576–82.
170. Jalalian A, Grishin AM. Piezoelectricity and electrostriction in biocompatible (Na, K)NbO_3 nanofiber scaffolds. *Appl Phys Lett* **2014**;*104*:243701.
171. Yousry YM, Yao K, Tan XL, Mohamed AM, Wang YM, Chen ST, Ramakrishna S. Structure and high performance of lead-free $(K_{0.5}Na_{0.5})NbO_3$ piezoelectric nanofibers with surface-induced crystallization at lowered temperature. *ACS Appl Mater Interfaces* **2019**;*11*:23503–11.
172. Xu XY, Liu YX, Lv Z, Song JQ, He MY, Wang Q, Yan LJ, Li ZF. Thermal study in Eu^{3+}-doped boehmite nanofibers and luminescence properties of the corresponding Eu^{3+}:Al_2O_3. *J Therm Anal Calorim* **2014**;*118*:1585–92.
173. Chen XQ, Wang Q, Wu X, Wang T, Tang YX, Duan ZH, Sun DZ, Zhao XY, Wang FF, Shi WZ. Piezoelectric/photoluminescence effect in one-dimensional lead-free nanofibers. *Scr Mater* **2018**;*145*:81–4.
174. Cui B, Chen ZH, Zhang QH, Wang HZ, Li YG. A single-composition $CaSi_2O_2N_2$:RE (RE=Ce^{3+}/Tb^{3+}, Eu^{2+}, Mn^{2+}) phosphor nanofiber mat: energy transfer, luminescence and tunable color properties. *J Solid State Chem* **2017**;*253*:263–9.
175. Zhou LX, Li D, Dong XT, Ma QL, Wang XL, Yu WS, Wang JX, Liu GX. $La_2O_2CN_2$:Yb^{3+}/Tm^{3+} nanofibers and nanobelts: novel fabrication technique, structure and upconversion luminescence. *J Mater Sci: Mater Electron* **2017**;*28*:16282–91.
176. Xu XT, Zhao SQ, Liang KY, Zeng JY. Electrospinning preparation and luminescence properties of one-dimensional $SrWO_4$: Sm^{3+} nanofibers. *J Mater Sci: Mater Electron* **2014**;*25*:3324–31.
177. Viswanathamurthi P, Bhattarai N, Kim HY, Khil MS, Lee DR, Suh EK. GeO_2 fibers: preparation, morphology and photoluminescence property. *J Chem Phys* **2004**;*121*:441–5.
178. Chetibi L, Busko T, Kulish NP, Hamana D, Chaieb S, Achour S. Photoluminescence properties of TiO_2 nanofibers. *J Nanopart Res* **2017**;*19*:129.
179. Lee KW, Kumar KS, Heo G, Seong MJ, Yoon JW. Characterization of hollow $BaTiO_3$ nanofibers and intense visible photoluminescence. *J Appl Phys* **2013**;*114*:134303.
180. Yu M, Dong RH, Yan X, Yu GF, You MH, Ning X, Long YZ. Recent advances in needleless electrospinning of ultrathin fibers: From academia to industrial production. *Macromol Mater Eng* **2017**;*302*:1700002.

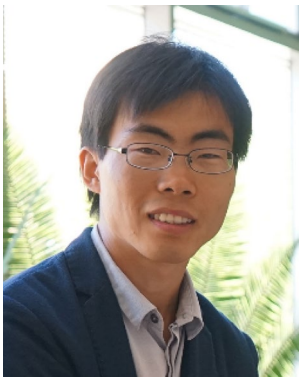

Chao Jia is an associate professor at College of Materials Science and Engineering, Donghua University. He obtained his Ph.D. degree from Beijing Institute of Technology in 2018. He worked as a postdoctoral research associate at Tsinghua University from 2018 to 2021. His research interests focus on nanofibers, cellulose nanomaterials, and wood-based functional materials.

Zhe Xu is a graduate student at College of Materials Science and Engineering, DongHua University under the supervision of Prof. Chao Jia. Her research interest is preparation and application of flexible ceramic fibers.

Dianfeng Luo is a graduate student at College of Materials Science and Engineering, DongHua University under the supervision of Prof. Chao Jia. His research interest is preparation and application of flexible ceramic fibers.

Hengxue Xiang is an associate professor at College of Materials Science and Engineering, Donghua University. He obtained his Ph.D. degree from Donghua University. His research focuses on the formation of functional fibers.

Meifang Zhu obtained her Ph.D. degree on Materials Science in 1999 from Donghua University (DHU, Shanghai). Currently, she is a professor at DHU and the member of Chinese Academy of Science. She also serves as the dean for the College of Materials Science and Engineering in DHU, and the director of the State Key Laboratory for Modification of Chemical Fibers and Polymer Materials. She has long been engaged in fundamental chemistry, properties, and applications research of fiber materials, organic/inorganic hybrid nano-materials, smart hydrogels and biomaterials for green energy, environment, and healthcare.